Presented at the International Conference on
Fundamental of Tribology, Massachusetts
Institute of Technology, Cambridge, Mass.
June 19-22, 1978

LBL-7328

AN INVESTIGATION OF TWO-BODY ABRASIVE WEAR

Howard H. Hirano and Alan V. Levy

April 1978

Prepared for the U. S. Department of Energy
under Contract W-7405-ENG-48

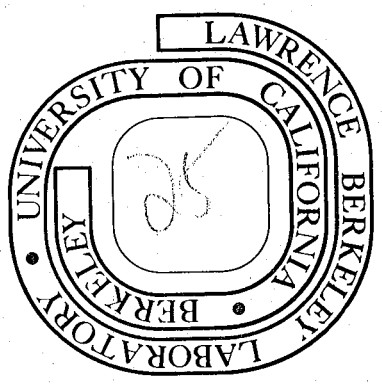

Presented at the International Conference
on Fundamentals of Tribology, Massachusetts
Institute of Technology, Cambridge,
Massachusetts, June 19-22, 1978.

LBL-7328

AN INVESTIGATION OF TWO-BODY ABRASIVE WEAR

By

Howard H. Hirano*

and

Alan V. Levy**

April, 1978

*Sandia Laboratories
Livermore, California

**Lawrence Berkeley Laboratory
University of California, Berkeley

ABSTRACT

An investigation of two-body abrasive wear utilizing a pin specimen on a rotating SiC particle abrasive paper test device is described. The test materials were 7075 aluminum and 4340 steel which were thermally treated to attain a range of hardness, fracture toughness and yield strength values. Wear resistance is seen to correlate directly with hardness and yield strength for both materials. For the 4340 steel the wear resistance is inversely proportionate to the fracture toughness; for the 7075 aluminum, the inverse proportionality is dependent upon the microstructure. The effect of an increase in hardness by heat treatment of an alloy is much less pronounced than when the wear resistance of pure metals of differing hardness are compared. Scanning electron microscopy of abraded surfaces was used to examine the removal mechanisms involved in abrasive wear. The meaning of the observed mechanisms in terms of a model are assessed.

ACKNOWLEDGMENTS

The guidance and support received from Professor Iain Finnie during the course of this investigation is gratefully acknowledged.

Appreciation is also expressed for assistance received from V. K. Pujari, M. S. Bhat, R. M. Horn, Don Krieger, Lee Johnson and Richard Lindberg in carrying out the investigation.

This work was supported by the Division of Materials Sciences, Office of Basic Energy Sciences, U. S. Department of Energy

TABLE OF CONTENTS

I. INTRODUCTION

The national energy policy calls for a greatly increasing use of coal. Many methods for producing liquid or gaseous hydrocarbons from coal have been proposed. Generally, these operate on a continuous basis and at pressures above atmospheric. The development of dry coal screw feeders to introduce coal into the process equipment has shown that abrasive wear problems may be a limiting factor in design. In addition, abrasive wear is a problem in other equipment for the transportation of coal as well as in mining machinery. These aspects were the motivation for the present study of abrasive wear.

Abrasive wear can be divided into two categories, two-body and three-body. Both types can occur in the coal energy conversion process. When abrasive grains are initially fixed onto one of the surfaces, two-body abrasion occurs (Fig. 1). Three body abrasion occurs when hard abrasive grains are introduced between surfaces whose hardness is significantly less than that of the abrasive (Fig. 1).

This paper is devoted primarily to a study of two-body abrasion as a first step in developing a more complete understanding of abrasive wear in coal conversion equipment. However, some comparisons are made with three-body wear results. There has been a considerable amount of work done in the area of two-body abrasion, much of it involving testing a wide range of materials and correlating the wear rate with other mechanical properties. The principal contribution of this type is the work of Kruschov[1]. His results (Fig. 2) have been verified by other researchers and are useful in establishing general trends in the wear resistance of certain types of materials.

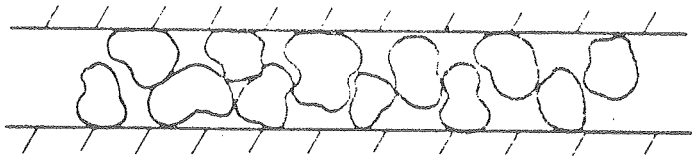

Three-body Abrasion

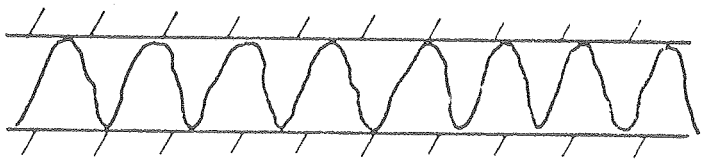

Two-body Abrasion

XBL 771-6443

FIGURE 1.

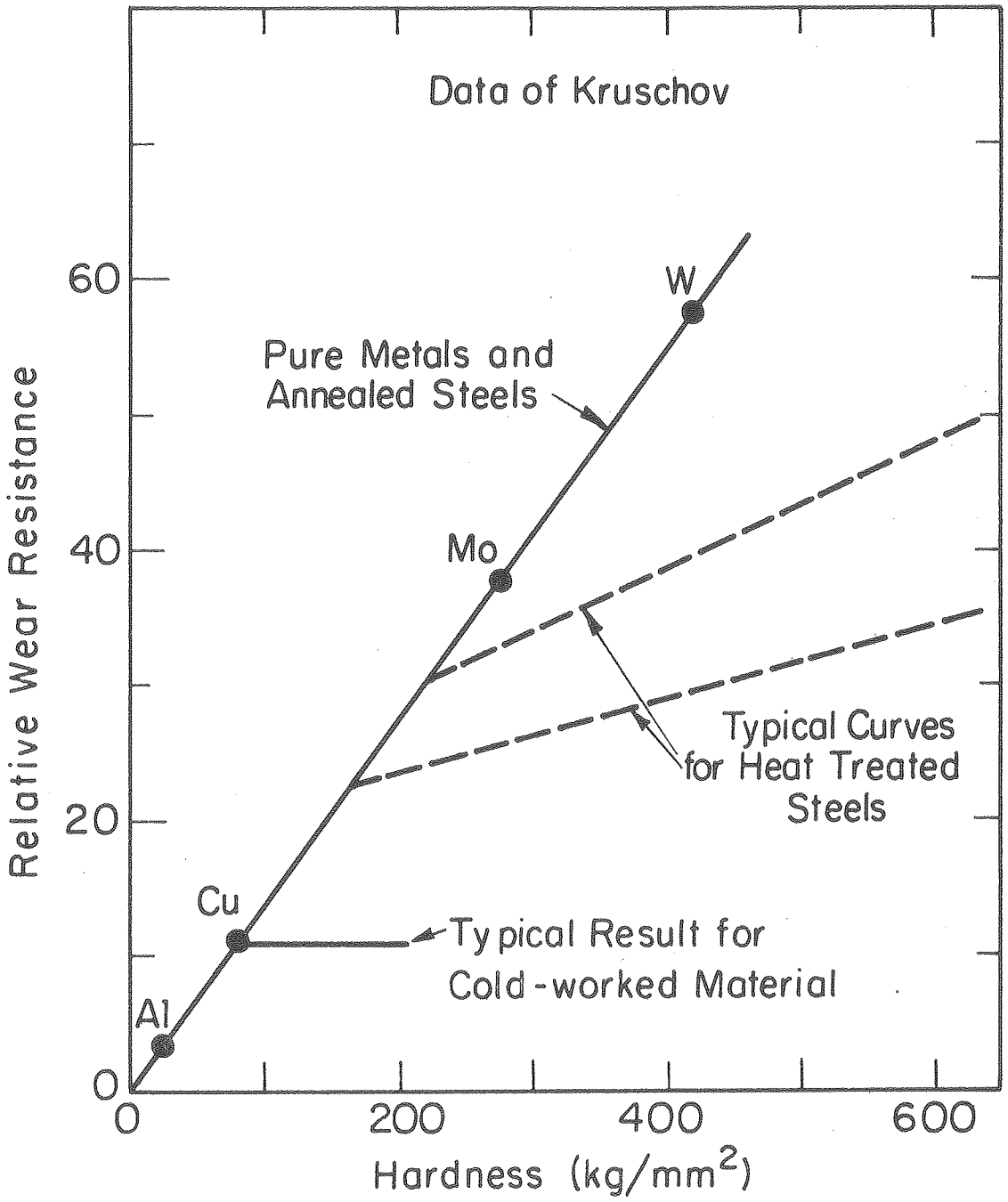

FIG. 2 - Summary of Data by Kruschov

Abrasive wear results are traditionally reported in several ways. One is the wear rate which is the volume removal per unit distance travelled per unit load. Alternatively, the reciprocal of this quantity may be used and is referred to as the wear resistance.

For pure metals and annealed steels, Kruschov found that the wear resistance was directly proportional to the Vicker's hardness of the material. As a steel was heat treated to increase its hardness, the wear resistance also increased. However, the increase in wear resistance was not as dramatic for a heat-treated steel as the increase in wear resistance of pure metals or annealed steels for the same increase in hardness.

In the case of cold-worked materials, little or no change was discerned in the wear resistance as a result of increases in the hardness due to cold-working. Kruschov concluded that the degree of strain hardening which occurs during the abrasion process is much greater than any initial work hardening and that this value of work hardening corresponds to the maximum level of hardness preceding destruction of the material.

Rabinowicz[2] developed a simple expression for the volume of material displaced by idealizing abrasive grains as being conical in shape (Fig. 3). He simply calculated the amount of material which would be displaced if the abrasive grain is dragged along the metal at some depth of penetration. Then, by noting the similarity between his expression and that for adhesive wear, he derived the following relation:

$$V = \frac{k\ L\ x}{3H}$$

where V = Volume displaced

L = Load

x = Distance travelled

H = Hardness of base metal

k = Dimensionless abrasive wear coefficient

While this equation is based on a simplified model, it does express some of the basic observations of both two-body and three-body abrasive wear. The volume of material removed is directly proportional to the load and distance travelled by the harder abrasive particle and is inversely proportional to the hardness of the softer abraded material.

Rabinowicz used this expression to compare the results obtained by a number of experimenters for two-body and three-body abrasion. The values of the abrasive wear coefficients were approximately an order of magnitude less for three-body than for two-body abrasion.

In addition to the simplification of the shape of the abrasive grain, the expression describes the total amount of material which is displaced from its original position in the softer material as being removed from the surface. This displaced material is not necessarily detached from the base material, as under some conditions it may be plastically deformed.

Mulhearn and Samuels[3] investigated the manner in which material is displaced. They identified ploughing and cutting as the primary modes of material displacement. The term "ploughing" is applied when material is plastically deformed by the abrasive grain. "Cutting" describes the situation where a chip is formed, as would be if the abrasive particle were replaced by a machine cutting tool. As a method of material removal, ploughing has a low efficiency, whereas almost all the displaced material in cutting is removed in the form of a chip.

Mulhearn and Samuels modeled the abrasive particle with a cutting

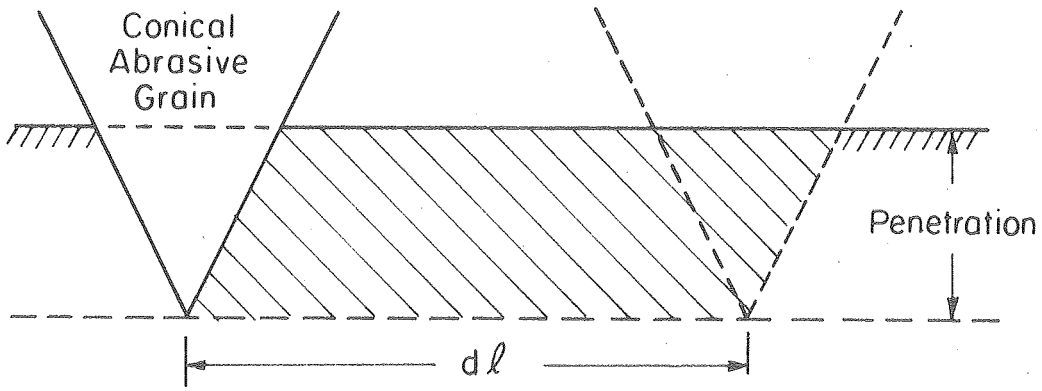

FIG. 3 Simple Model of Abrasion by Rabinowicz

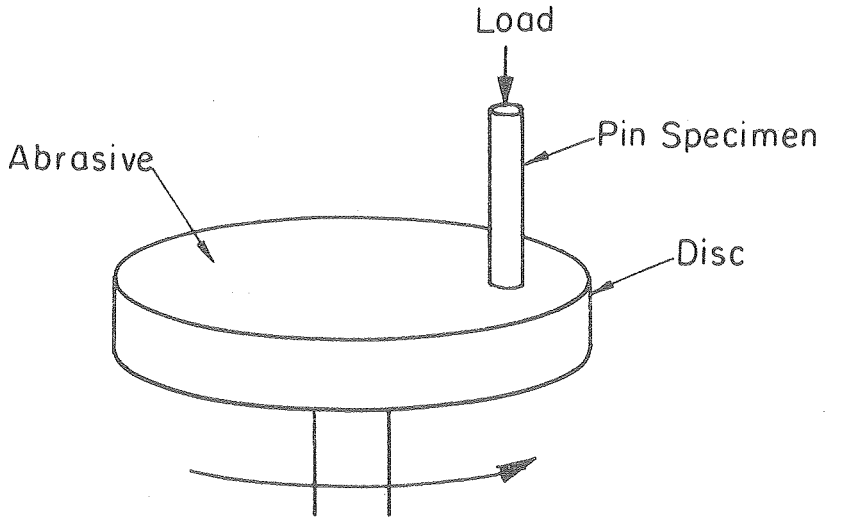

FIG. 4 Pin on Disc Abrasion Tester

tool and studied the effect of the orientation angle of the tool to the base metal. The critical value of this angle, which they termed the "critical attack angle," determined whether cutting or ploughing occurred. Angles greater than the critical value resulted in ploughing; whereas, cutting occurred for smaller angles. From their tests, the critical attack angle measured from the plane of the abraded surface to the tool face was found to be 90°.

Mulhearn and Samuels also spent a good deal of time characterizing abrasive grains and the abrasive papers used in two-body abrasion tests. Among their results is the number of abrasive grains which contact the surface of the abraded material and actually cut. They determined this number to be 12% for the loading and particle size distribution they studied.

Numerous other investigations of abrasive wear include studies of the hardness ratio of the abrasive to the abraded material[1,4]; the effect of specimen size[5]; and the effect of abrasive grain size[6,7] and shape[8].

II. EXPERIMENT

A. Wear Tester

The most common type of two-body abrasion tester is the simple pin on disc machine (Fig. 4). Abrasive, normally in the form of abrasive paper, is fixed onto the top surface of the rotating disc. The head of the pin specimen is held against the abrasive, usually by dead weight loading. As the disc is rotated at a fixed speed, the head of the specimen is abraded. In most cases the pin is allowed to traverse radially inward during the course of the test. This allows the pin to be continually exposed to fresh abrasive.

The testing apparatus used for this investigation was of the type described above. A strain gauge ring was also included to allow measurement of the friction coefficient during sliding abrasion. For most of the testing, Carbimet Silicon Carbide Abrasive Papers with Pressure-Sensitive Adhesive backing were used.

The overall view of the abrasive wear tester is shown in Fig. 5. The test area of the pin-on-disc test configuration is observed in Fig. 6. The specimen is a 1/4-inch-diameter pin with an 1/8-inch radius or curvature at the contact end. The disc, which has a diameter of 4 inches, has a SiC bonded abrasive disc placed on it. It is given a rotary motion and the pin can be kept stationary or moved radially on the disc. When the pin is stationary the same track will be traversed on the disc; however, for the radial motion of the pin, the contact path on the disc is a spiral and a fresh area of the disc will be in contact with the pin after each revolution.

The close-up of the pin holding section and abrasive disc of the abrasive wear tester is shown in Fig. 7. The pin assembly is also used to apply the normal contact load and to measure the frictional force. The normal load on the specimen is applied by attaching weights to the weight pan and will be varied to simulate in-service loads. The frictional force is measured by means of a strain ring arrangement. The strain ring is designed to be flexible and deform elastically under the action of the frictional force. This deformation is measured by strain gauges attached to the ring and is monitored through the recorder to indicate the frictional force. The pin holder and strain ring assembly are connected to a pair of pillow blocks. The weight of the assembly

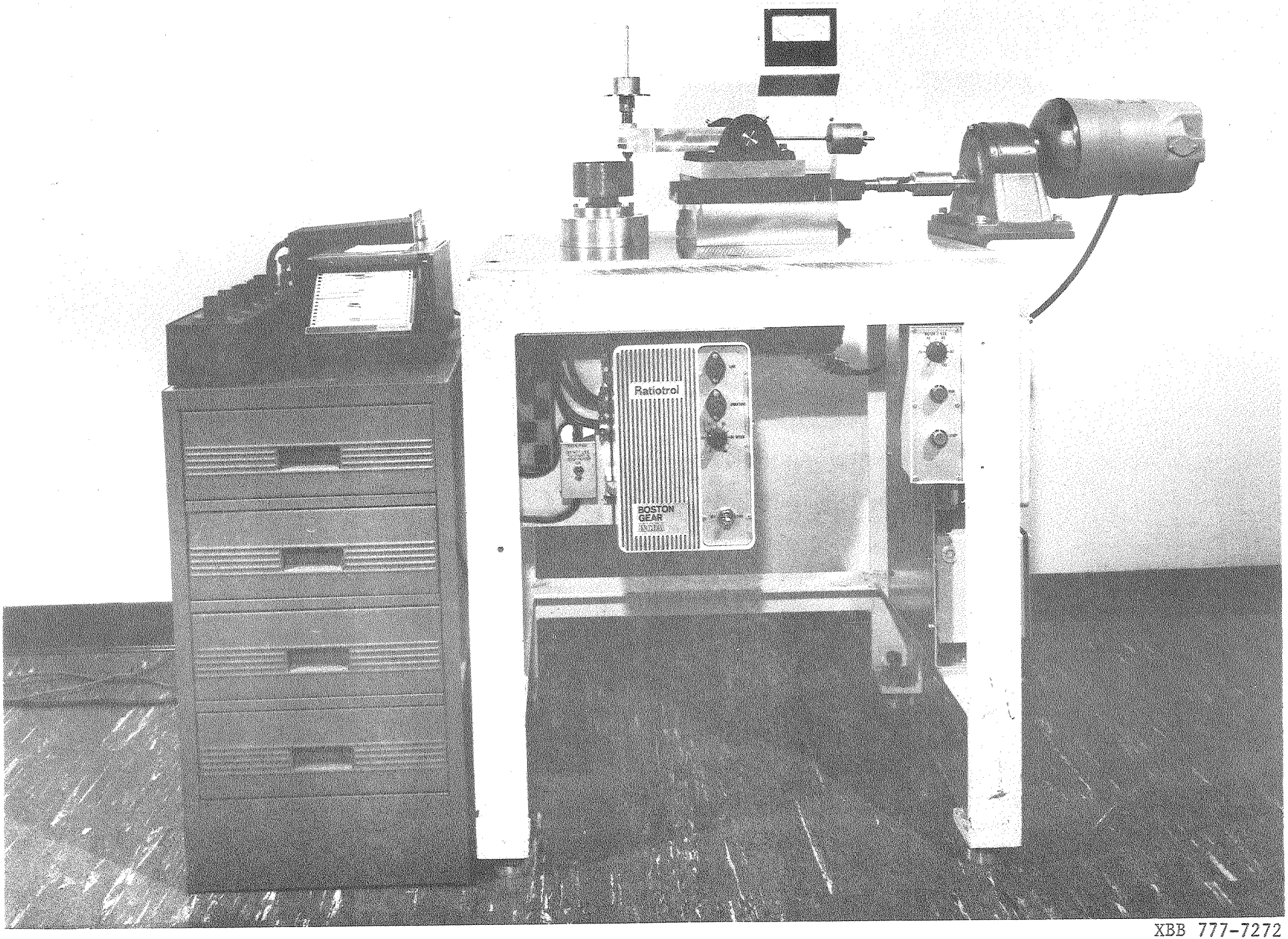

XBB 777-7272

FIGURE 5. Overall View of Dry, Abrasive Wear Tester

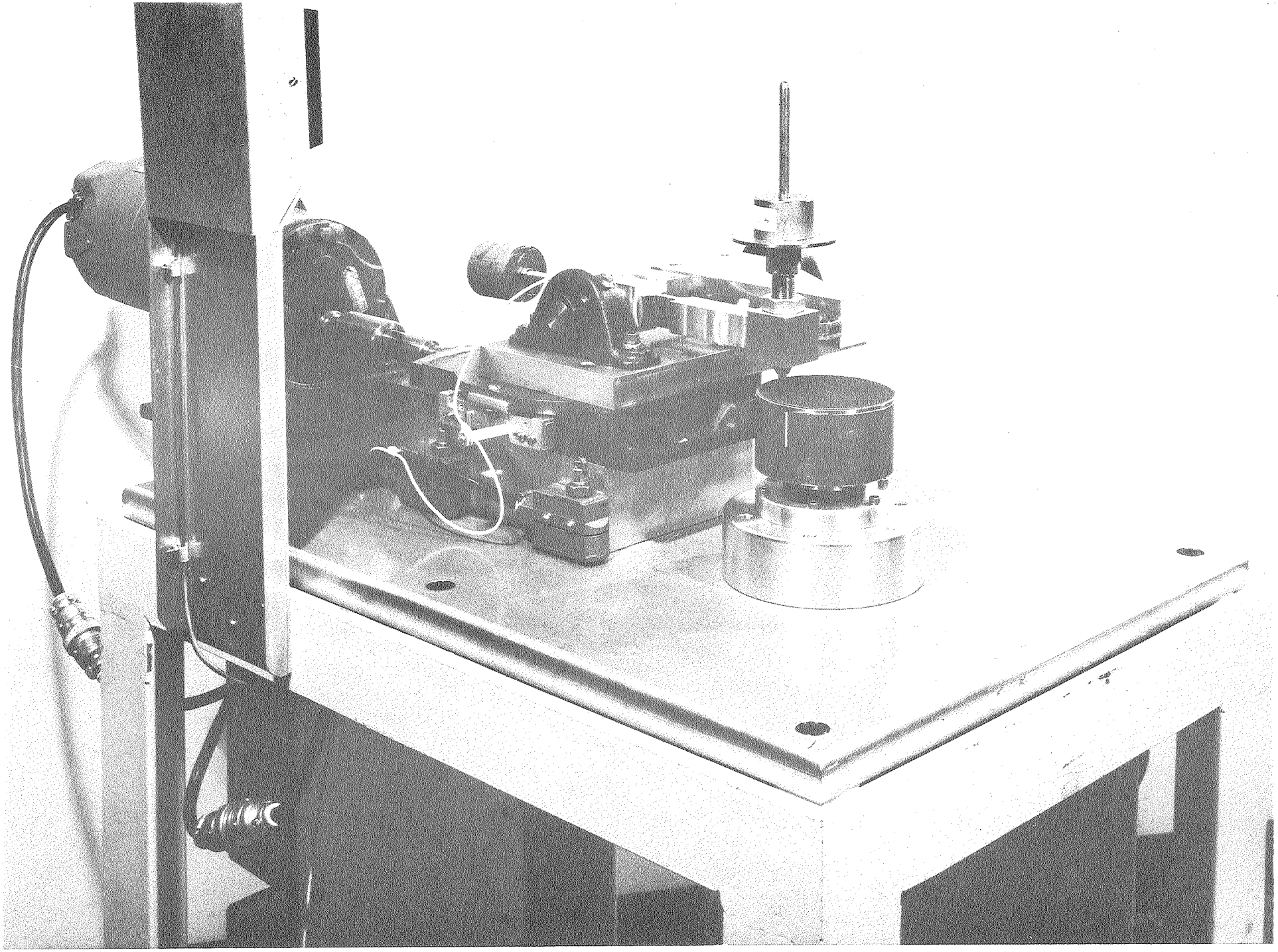

FIGURE 6. View of Test Area of Dry, Abrasive Wear Tester.

XBB 777-7274

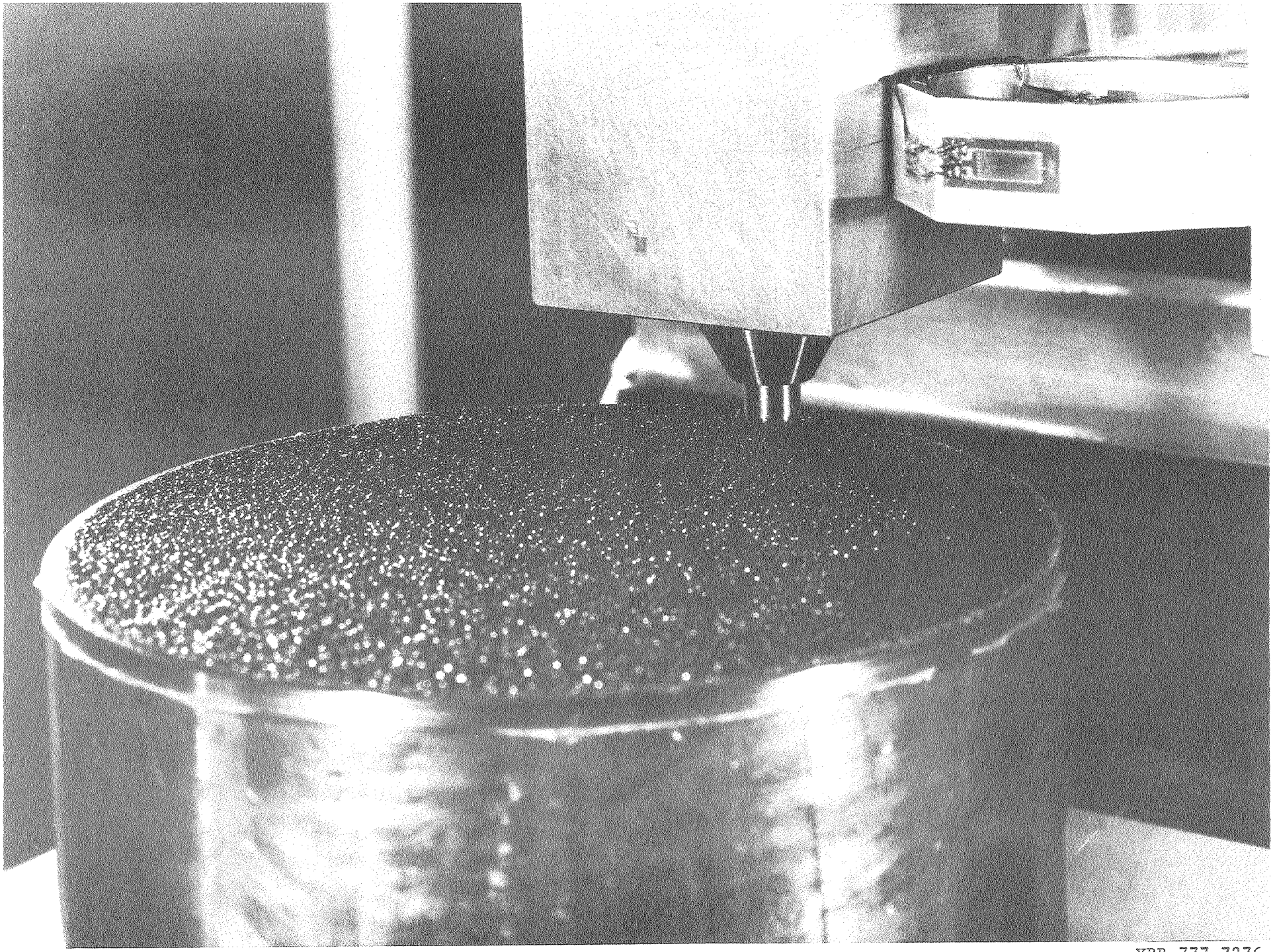

FIGURE 7. Close-up of Pin and Abrasive Disc.

XBB 777-7276

is balanced by the counterweight. This assembly is attached to a tracking mechanism to provide the radial motion of the pin on the rotating disc.

The abrasive wear tester has been designed to operate at room temperature; however, modifications are possible for elevated temperature tests. The maximum normal load is 20 pounds, which is great enough to simulate in-service loads. The speed range of the turntable is between 20 to 200 rpm which gives a maximum speed of 2,500 in/min at the contact with a 4-inch disc. In order to achieve higher speeds the turntable can be made larger. The maximum allowable diameter of the turntable is 8 inches.

Unless otherwise noted, the specimens were dead weight load with 500 gm against 120 grit silicon carbide abrasive paper. All of the tests comprising this investigation were performed at the same, constant speed of rotation of the disc (20 rpm) for 45 seconds.

The mechanism which controls the radial traversing of the specimen was adjusted so that all of the specimens travelled from 1.8 inches radius to .54 inch radius in the 45 seconds. Thus, all of the specimens were abraded for the same distance which was determined to be 2800 mm. The average velocity of the abrasive relative to the specimen was 6.2 cm/sec. The abrasive paper was changed before each test and examination of the wear track on the paper indicated that the radial traversing speed was adequate to insure that the specimen was continually exposed to fresh abrasive.

Wear rate was reported as volume of metal lost per unit distance travelled, in mm^2. The inverse of this number was used in the curves to

designate erosion resistance. Since a fixed load of 500 gm was used for all of the tests, the load was not used to calculate the wear rate.

B. Wear Test Specimen

The specimens were 0.25 in. diameter by 0.70 in. long. The end of the specimen which was to be abraded was machined hemispherical to discourage any initial effects due to misorientation. After machining, the specimens were lightly buffed with 600 grit silicon carbide abrasive paper.

The primary materials of interest for this investigation were 7075 aluminum and 4340 steel. Both of these materials were heat treated to various levels of hardness, fracture toughness and yield strength to study the effect of these mechanical properties on abrasive wear resistance.

The 7075 Al was obtained from two previous investigations of the effect of heat treatment on the fracture toughness of the alloy.[9,10] The fracture toughness specimens used in these investigations were 1 inch by 20 inch by 10 inch plates which were differentially heat-treated by means of strip heaters. In this manner, heat-treated conditions in both underaged and overaged from the optimal T-6 condition were obtained.

The wear specimens made from the eight overaged conditions tested in this program were machined from the grip ends of broken tensile specimens. The values of fracture toughness and yield strength used for this investigation were as reported by Pujari.[9]

In the case of the underaged material, four conditions were selected. Tensile and wear specimens were machined from the original fracture specimen. The specimens were machined such that the cylindrical axes were transverse to the rolling direction of the plate, in order to be

consistent with the overaged material. The fracture toughness values used were as reported by Shenai,[10] while the yield strength values were obtained from the tensile specimens.

To perform hardness tests on both overaged and underaged material, a 0.25 inch thick slice of material was removed from the wear specimens.

The mechanical properties of interest for the 7075 Al wear specimens are listed in Table I.

The 4340 steel was obtained in the form of Charpy specimens from a previous investigation. These notched bar specimens were first heat-treated at 675°C to that they could be machined. The wear specimens were then machined from this material to 0.040 inches oversize on the diameter. The oversize specimens were austenitized at 870°C and then oil quenched. Four tempering treatments were selected: 200°C, 350°C, 500°C, and 650°C. The tempering treatment was performed in a neutral salt bath followed by a water quench. Following the tempering treatment, the wear specimens were ground to the final dimensions.

The mechanical properties of interest for the 4340 steel are listed in Table II.

III. RESULTS AND DISCUSSION

A. Load and Abrasive Particle Size Effect

Several tests were conducted to compare the wear data obtained in this investigation with values observed by other experimenters.

The wear rate was, as expected, directly proportional to the load applied on the specimen (Fig. 8). The graph connecting the data points does not pass through the origin. This is attributed to the specimen

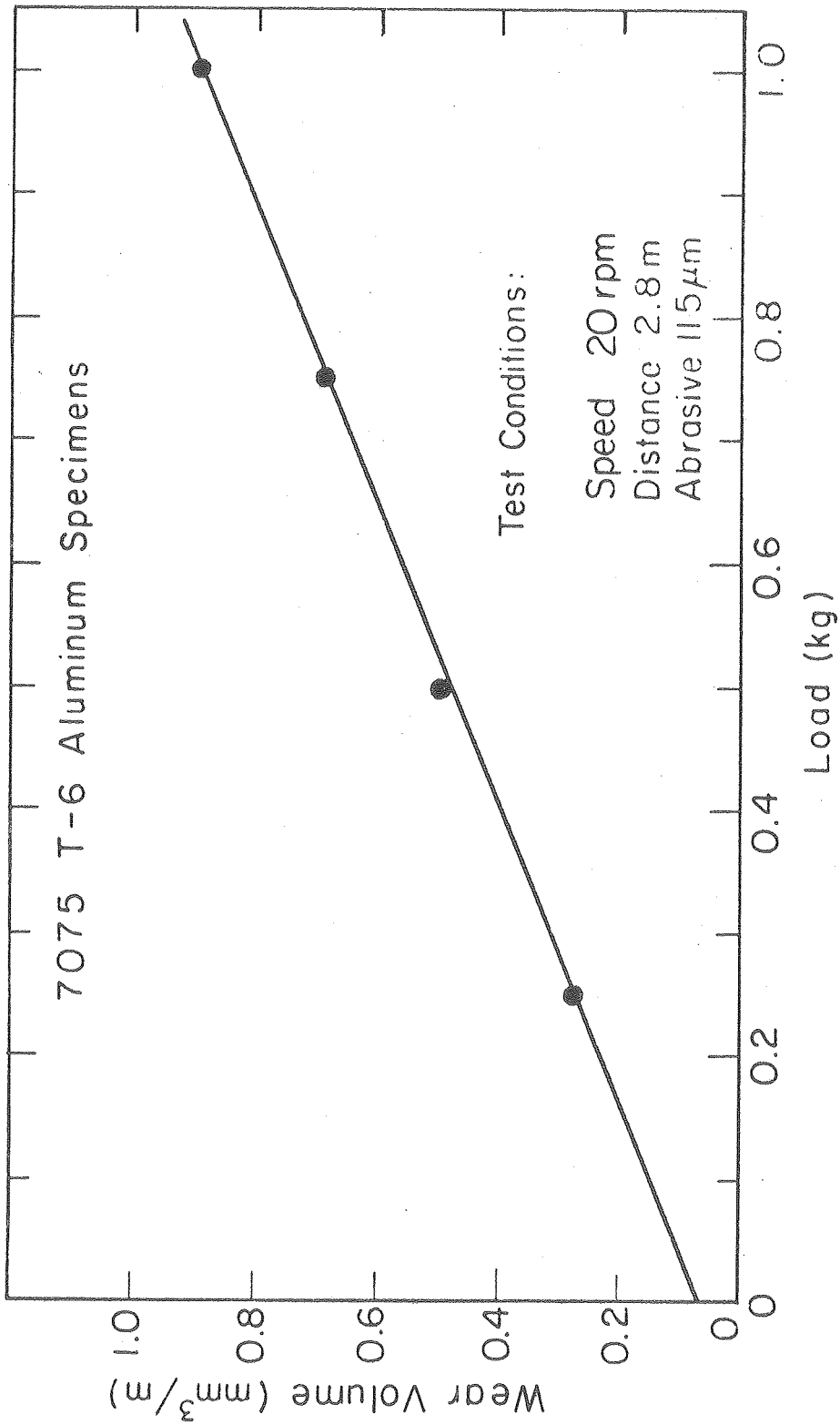

XBL 7711-6440A

FIGURE 8. Effect of Load on the Wear Rate of 7075-T6 Aluminum.

support arm of the wear tester not being in perfect balance. While attempts were made to reduce this effect, all of the later testing on the heat-treated 7075 Al and 4340 steel were conducted at a large enough load level so that the error due to the uncertainty in load was less than ten per cent.

The effect of the abrasive particle size is an interesting one which has received some attention. The particle size above which no significant effect is seen was ~ 100 μm (Fig. 9). This is the same size which has been noted by others for two-body abrasion[7]. The same result has also been reported for erosion[13]. The weight loss measured when using ~ 265 μm Sic abrasive particles may have been affected by the bonding technique used in the abrasive paper. Therefore, that data point was neglected in establishing the general trend discussed above.

This is a difficult effect to consider and warrants an investigation of its own. For the purpose of investigating the effect of the mechanical properties of the base metal, it was decided to simply use a fixed abrasive size for all the tests. This size (~ 115 μm) was chosen to lie in the region for which no grain size effect is expected.

B. Effect of the Mechanical Properties of 7075 Al and 4340 Steel

The wear resistance of 7075 Al is shown as a function of hardness, yield strength and fracture toughness in Figs. 10, 11 and 12. The same information is shown for the 4340 steel in Figs. 13, 14 and 15.

For the purpose of establishing any kind of correlation, hardness and yield strength seem to be good measures of the wear resistance. For 7075 Al, there was less scatter in the general trend of the data with

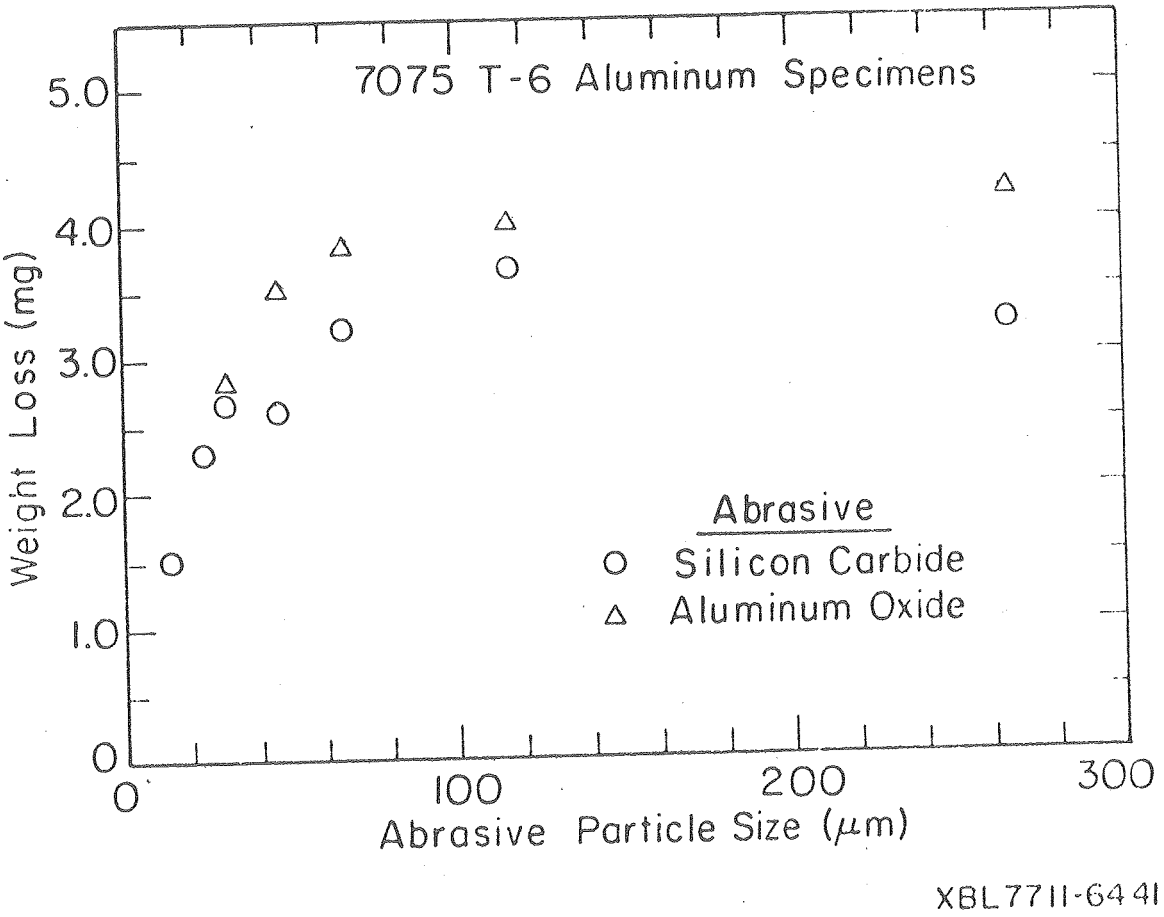

FIGURE 9. Effect of Abrasive Particle Size on the Wear Rate of 7075-T6 Aluminum.

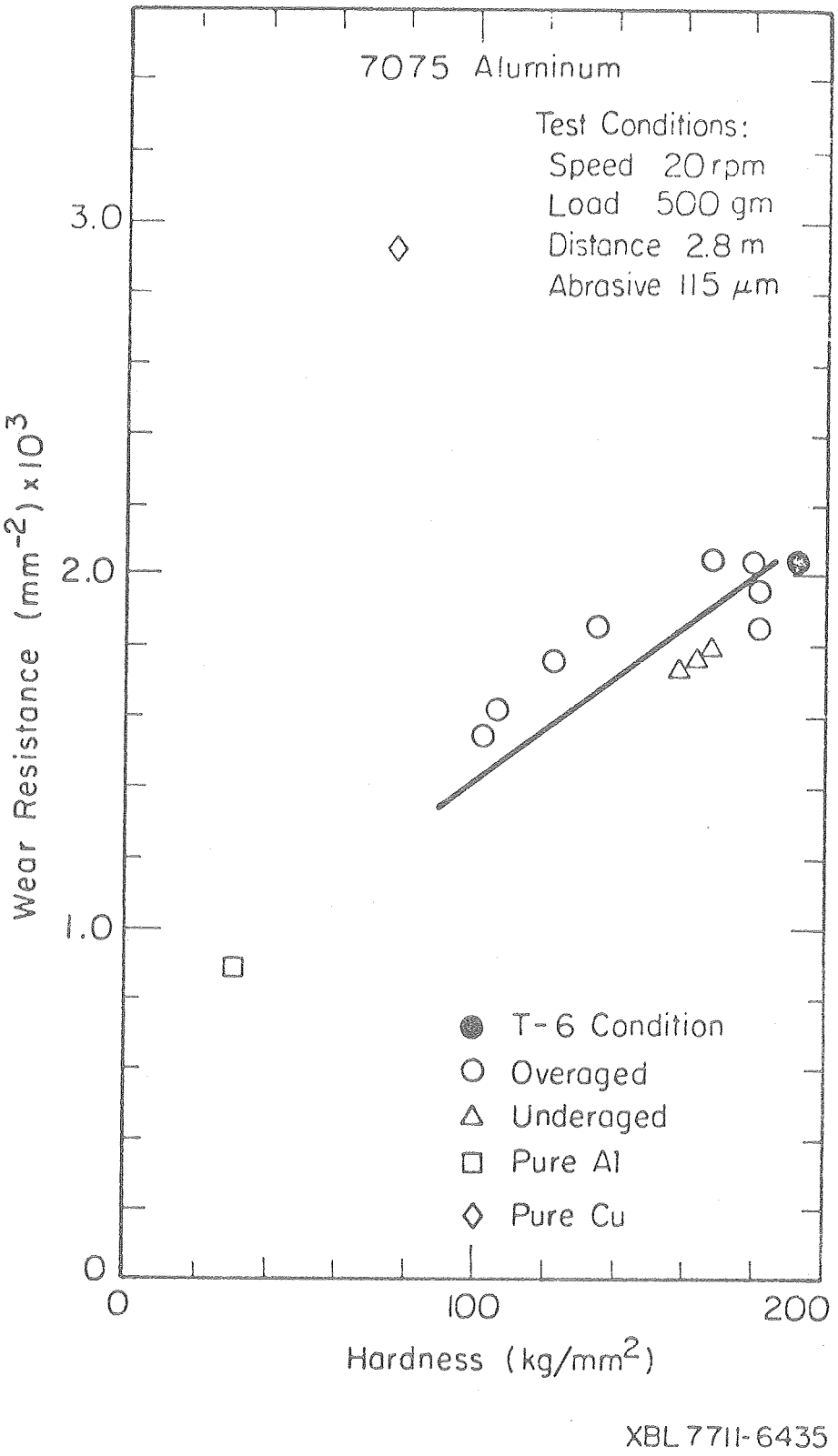

FIGURE 10. Wear Resistance of 7075 Al vs. Hardness

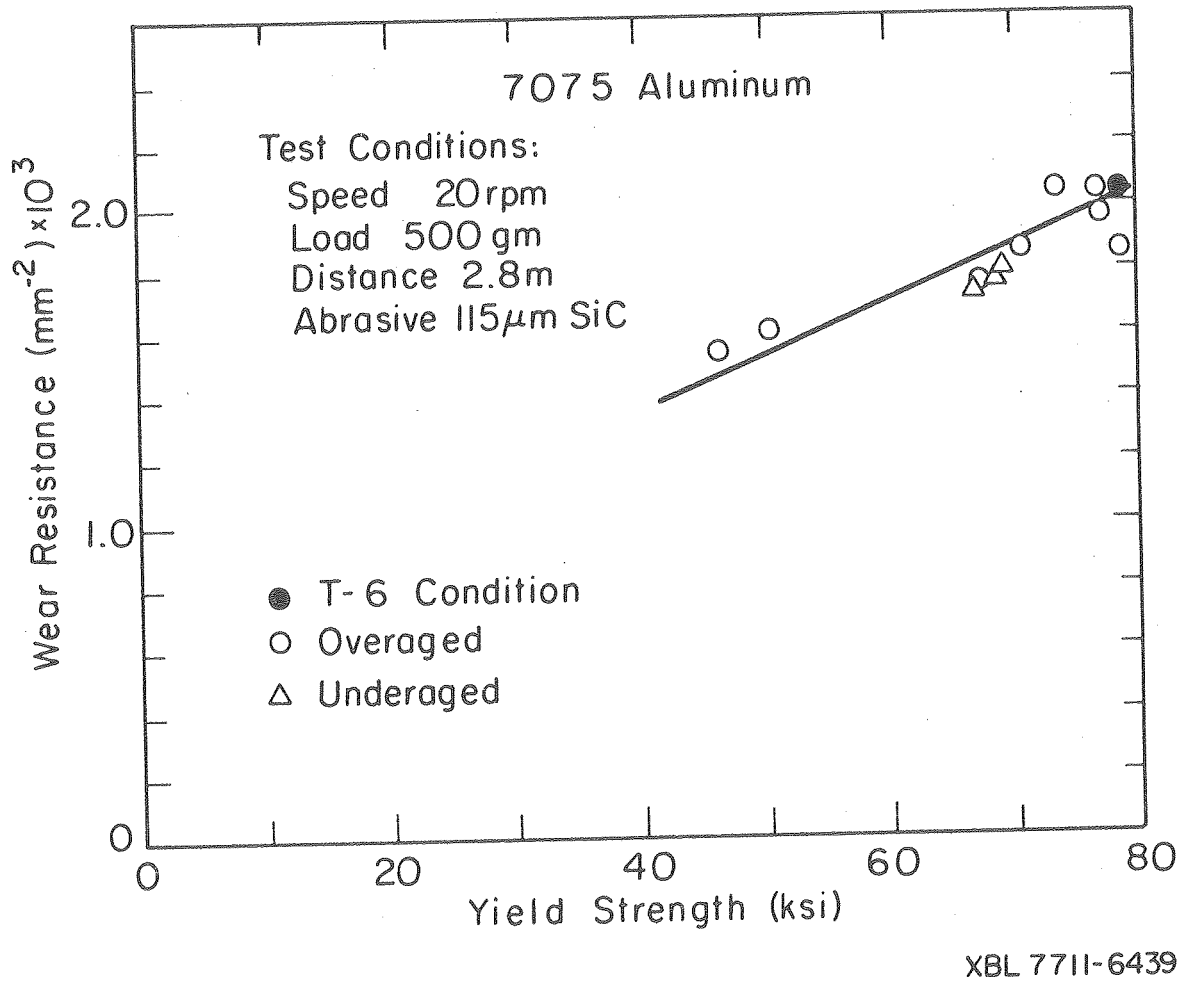

FIG. 11 Wear Resistance of 7075 Aluminum vs. Yield Strength

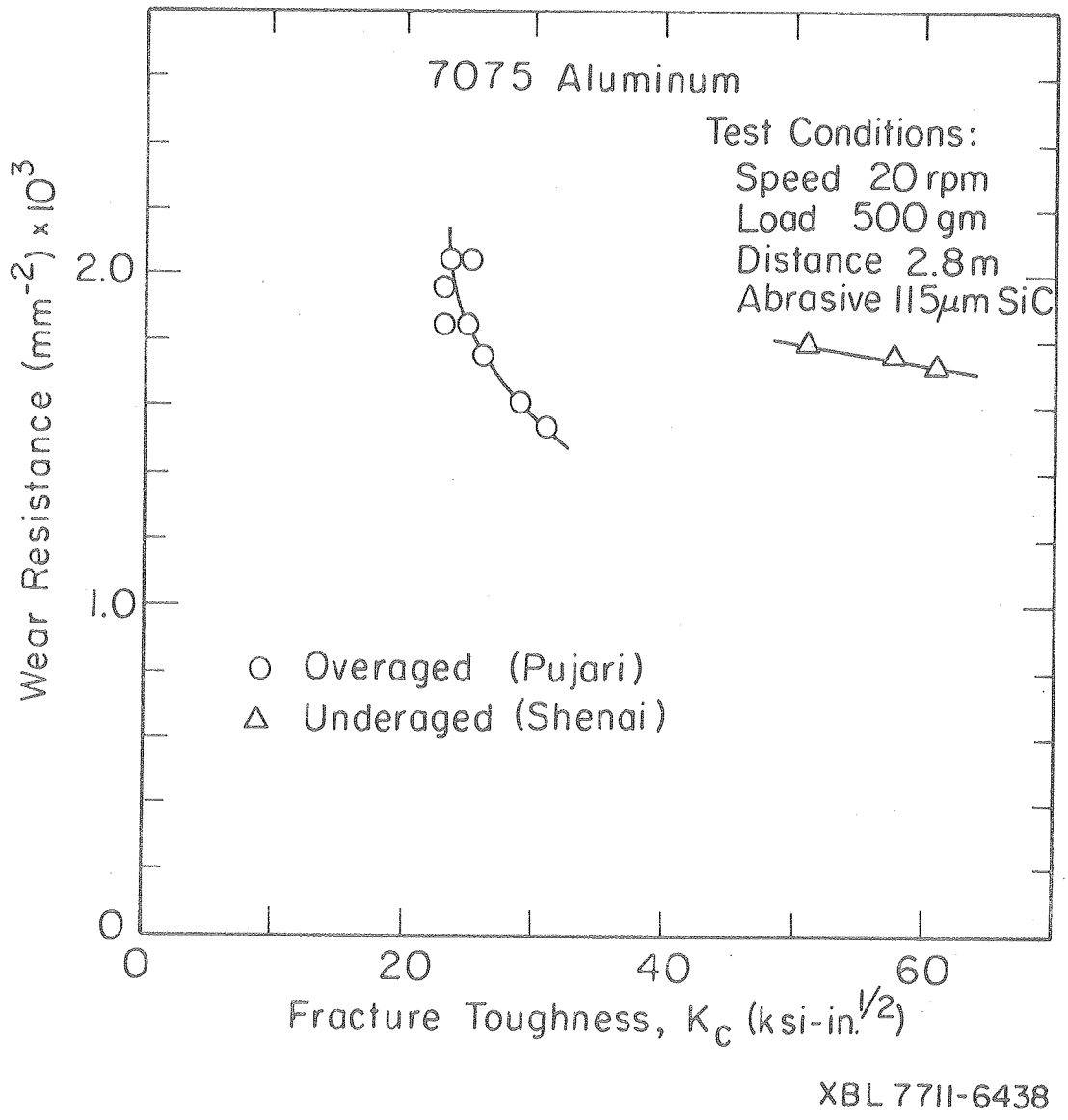

FIG. 12 Wear Resistance of 7075 Aluminum vs. Fracture Toughness

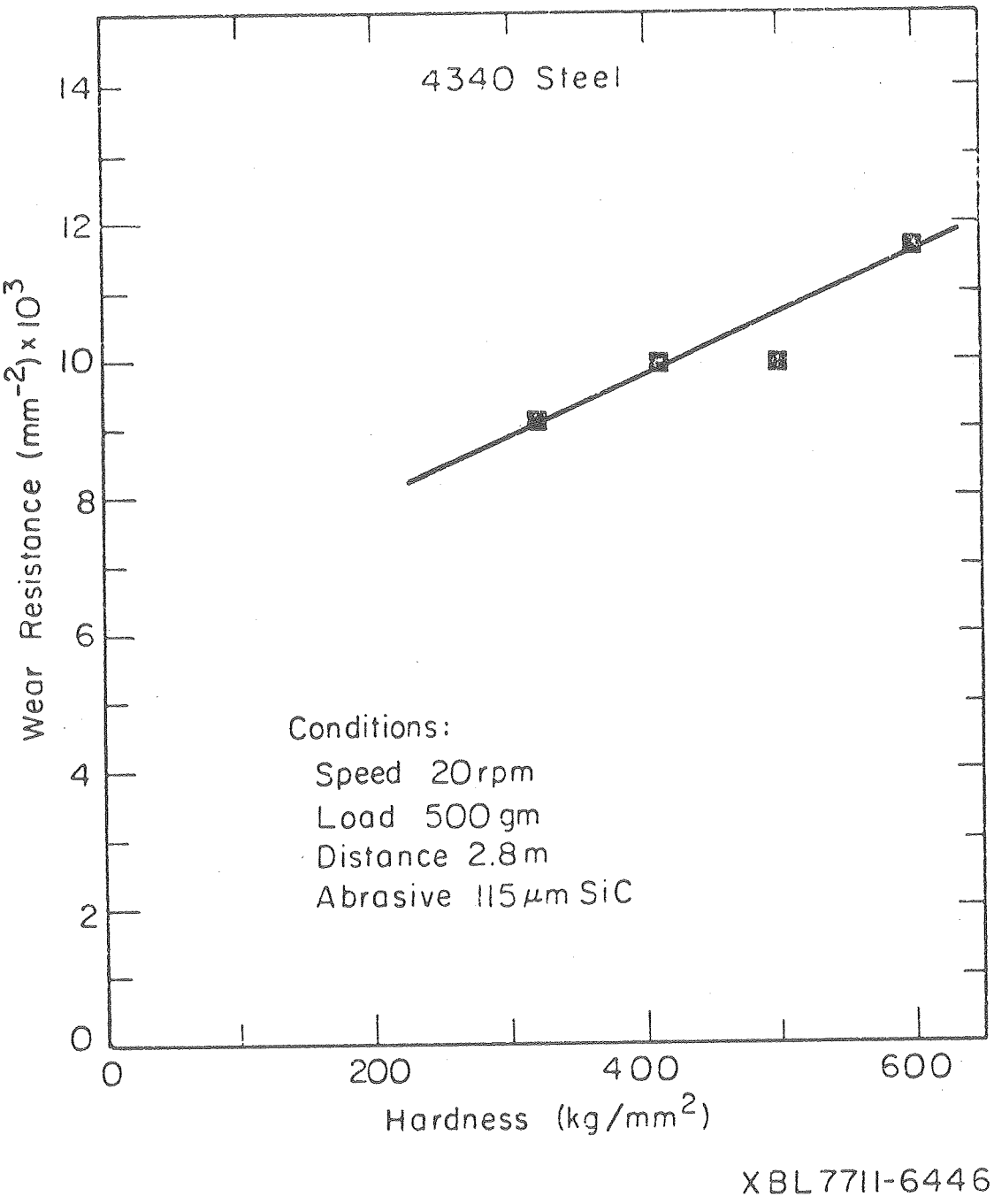

FIGURE 13. Wear Resistance of 4340 Steel vs. Hardness

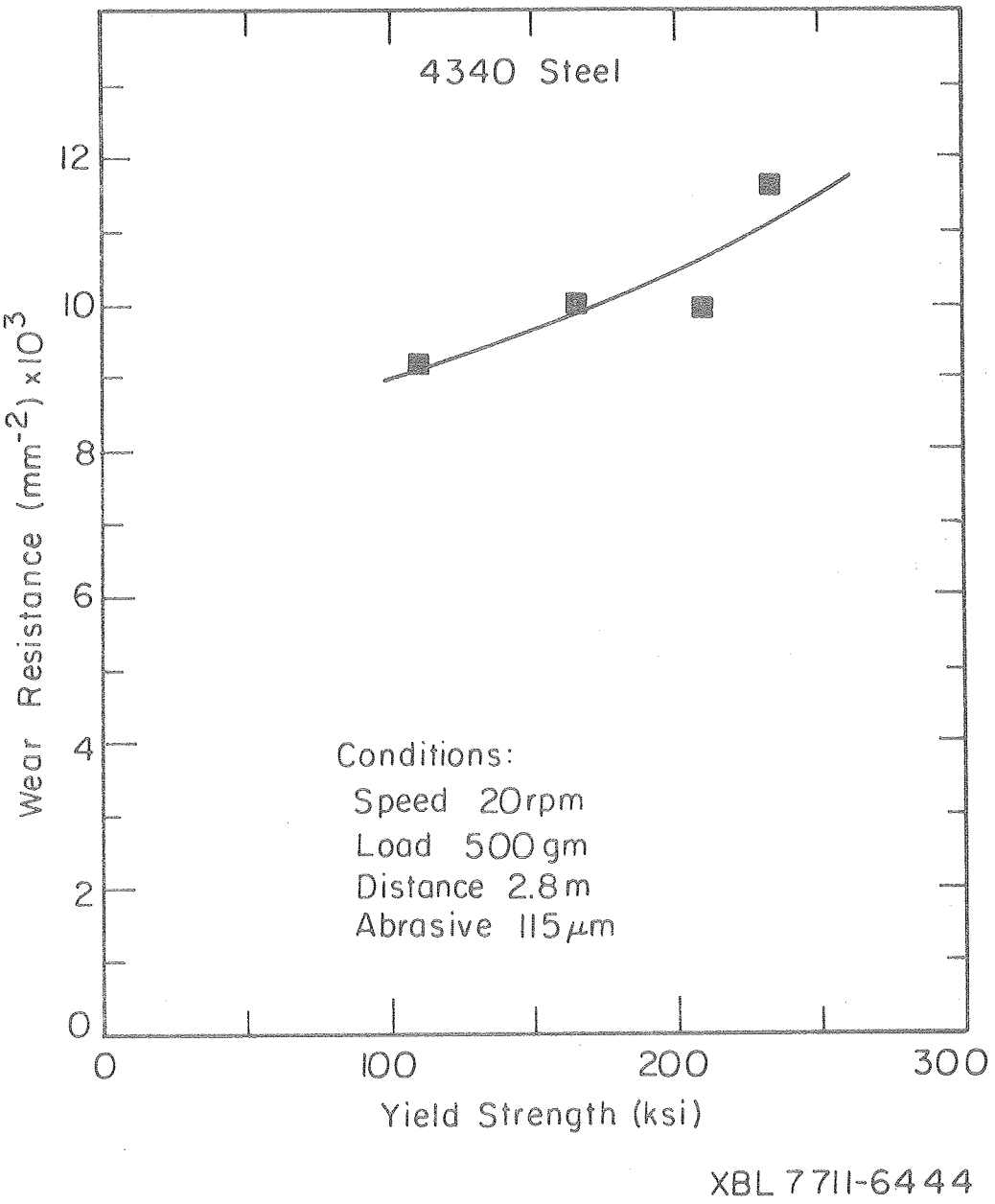

FIG. 14 Wear Resistance of 4340 Steel vs. Yield Strength

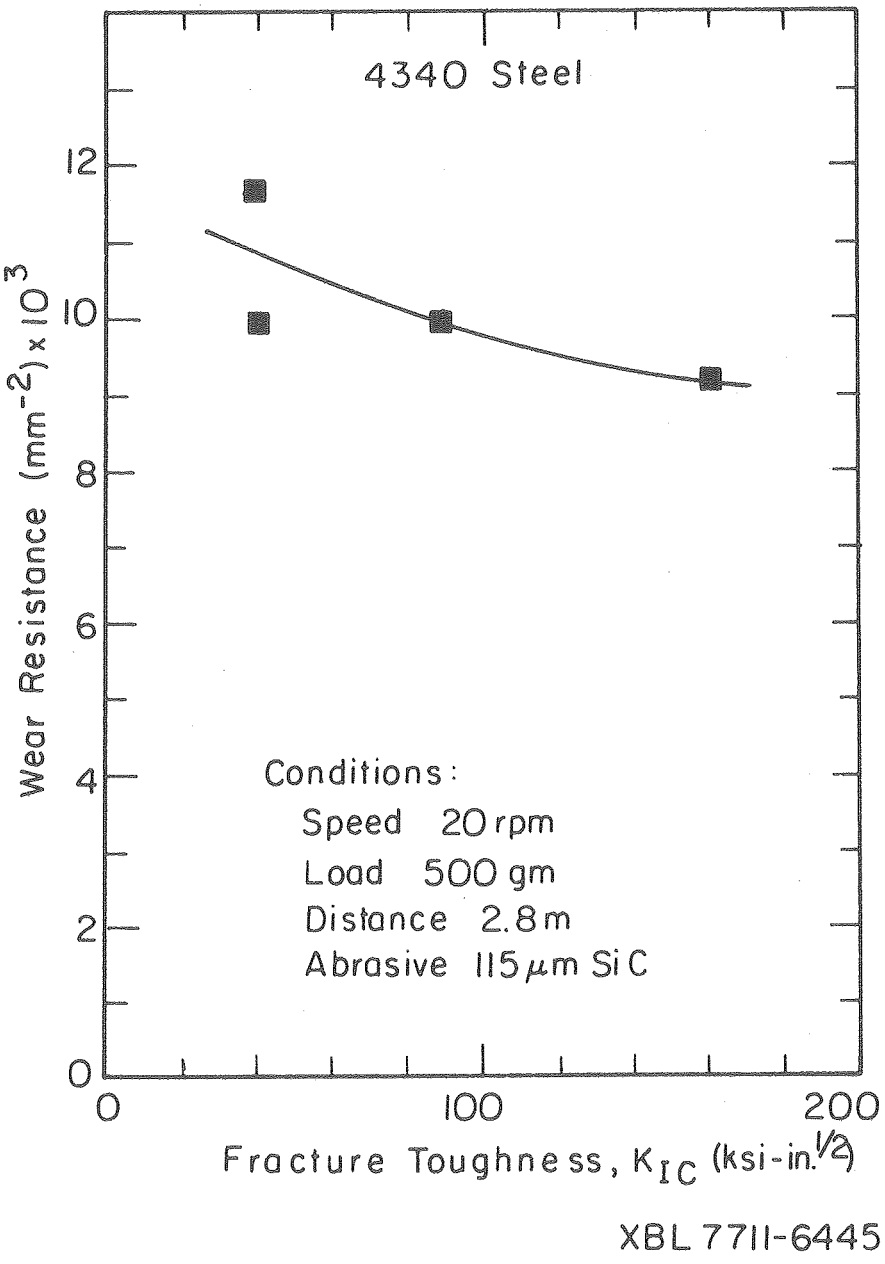

FIG. 15 Wear Resistance of 4340 Steel vs. Fracture Toughness

yield stress than with hardness. However, one would expect the general trends associated with hardness and yield strength to be similar since both quantities are measures of the resistance to plastic flow in a metal. No single correlation could be seen as a function of the fracture toughness for the 7075 Al. It appears from Fig 12 that the overaged and underaged structures each has a different relation between fracture toughness and wear. The wear resistance of the 4340 steel also has a correlation with the fracture toughness. It is interesting to note that the wear resistance decreases with increasing fracture toughness, the opposite effect of what one would suppose. The implications of this require further study. The difference in hardening mechanism and microstructure between the two types of alloys is significant and could account for the fracture toughness correlation difference.

Figure 16 shows the wear resistance of the 7075 Al and 4340 steel as a function of hardness. From this figure it can be seen that the general effect on the wear resistance due to increases in hardness as a result of heat treatment for the 7075 Al is remarkably similar to that for the 4340 steel. This effect is consistent with that reported by Kruschov for heat treated steels. While the wear resistance does increase with hardness, the amount of increase is much less than for the same increase in hardness in pure metals. In the case of the 7075 Al, doubling hardness resulted in an increase in the wear resistance of ~ 35%. For the 4340 steel, doubling the hardness increased the wear resistance ~ 30%.

Using Rabinowicz's model and the values of the abrasive wear coefficient which he calculated using the data which other workers reported for many materials (Table III), lines representing this data are also

included in Figure 16. For comparing to the data of this investigation, the line representing Spurr should be better since the abrasive particle size is above the critical size for no size effect, and the size is approximately the same as the 115 μm particles used in this investigation. From these lines, it is seen that for the many materials studied by Spurr a two-fold increase in hardness would result in an increase in the wear resistance of approximately the same magnitude.

C. SEM Examination of Wear Specimens

Aghan and Samuels[14] compared abrasive polishing (fine abrasive smaller than 8 μm) to abrasion (abrasives larger than 10 μm). Among their conclusions was that the mechanisms of material removal were similar, only the scale differed. Looking at Figures 17 and 18, it is easy to justify expanding this conclusion to two-body abrasion in general. The specimens in both figures were 7075-T6 Al tested under identical conditions with the exception of the abrasive particle size. The specimen in Figure 17 was abraded against ~ 14 μm particles while that in Fig. 18 was abraded against ~ 115 μm abrasive. In Figs. 17 and 18 the horizontal lines represent wear tracks which start at the juncture of those lines and the vertical polishing marks.

Fig. 19 shows a 4340 steel specimen whose hardness is approximately three times that of the 7075 Al. The test conditions for the 4340 sample were the same as that of the 7075 Al specimen in Fig. 18. From close examination of these three figures it can be seen that the basic material removal process is the same. Returning for the moment to Fig. 3 (Rabinowicz's simple model), decreasing the abrasive particle size

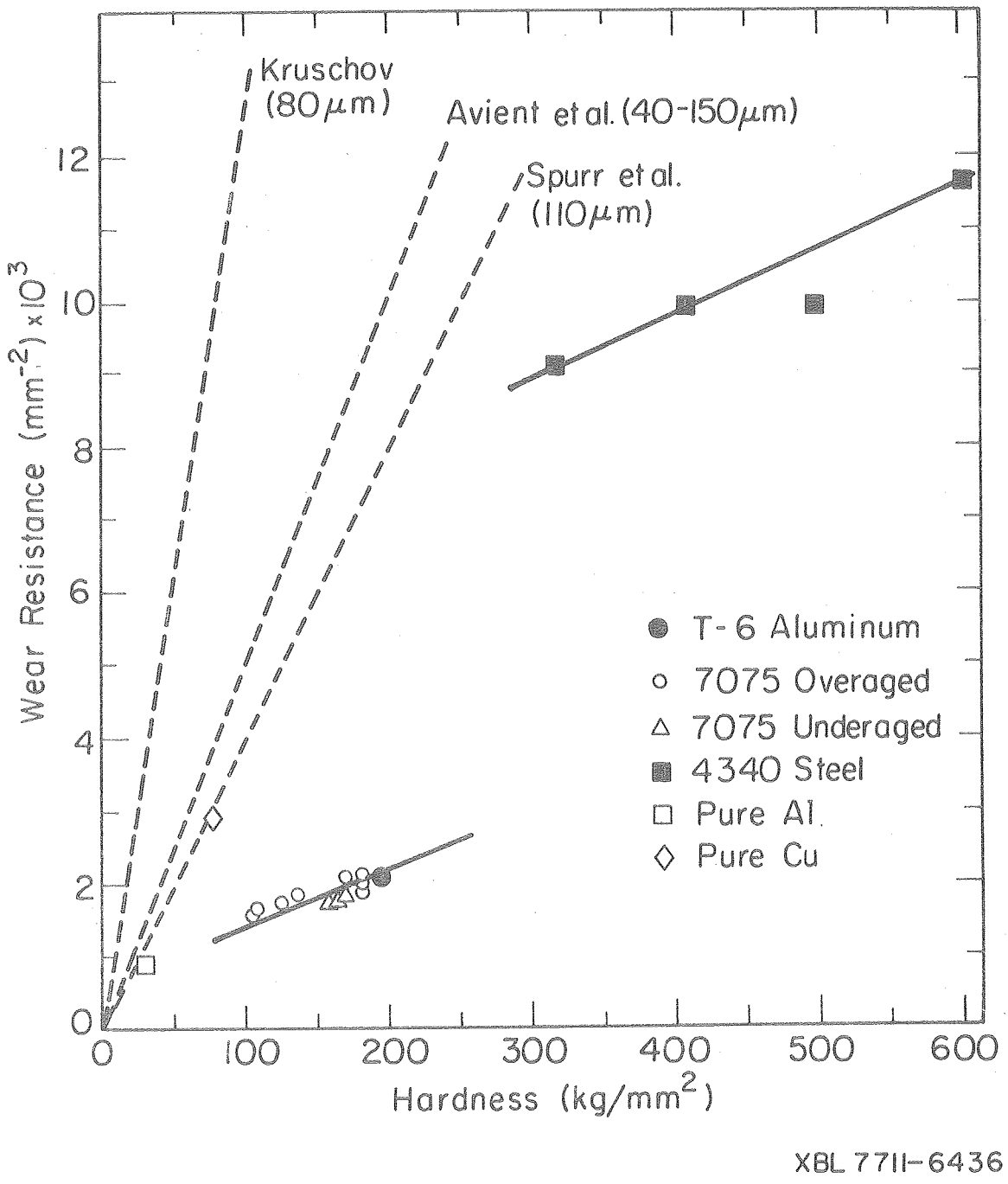

FIG 16 Comparison of Wear Resistance of 7075 Aluminum and 4340 Steel

would indicate the same material removal mechanism but on a smaller scale. This is consistent with the observations of Figs. 17 and 18. Increasing the hardness of the base metal would mean that the abrasive particle should penetrate less into the base metal for the same loading of the pin. This also indicates that the same type of material removal mechanism occurs, but on a smaller scale. This is consistent with the comparisons of Figs. 18 and 19.

Rabinowicz's model assumes that when material is displaced, it is cut cleanly away, with no chips remaining and no plastic deformation. However, looking at Fig. 20, at least three very obvious mechanisms of material displacement can be identified. These are plastic flow, cutting and gouging. The plastic flow mechanism is indicated by the raised ridges found at the edges of the grooves. The presence of cutting chips indicates that a cutting process occurs and the large pit in the lower portion of the photo testifies that a gouging mechanism is responsible for at least some of the material removal.

Fig. 21 is of a specimen abraded under the same conditions as that of Fig. 20 with the exception that the load was doubled to 1000 gm. Both of these photographs were taken at the trailing edge of the specimen. Because of the location it is probable that the gouging which is seen occurs when abrasive grains are fractured or pulled out of the paper, embedded in the softer material and pulled out by succeeding particles which are still attached to the paper. Figs. 17, 18 and 19 were taken at the leading edge of the specimen and do not show signs of gouging. Generally, gouging does not appear until somewhat past the leading edge.

Plastic flow at first appears to be the only mechanism present if one

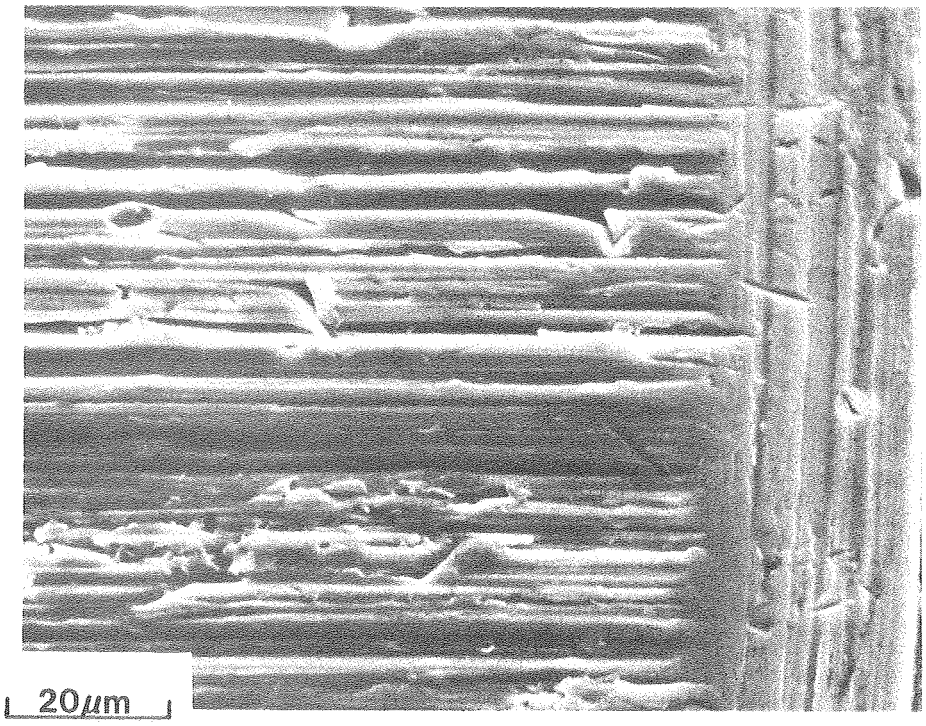

FIGURE 17. 7075-T6 Aluminum Abraded on ~ 14 μm Abrasive

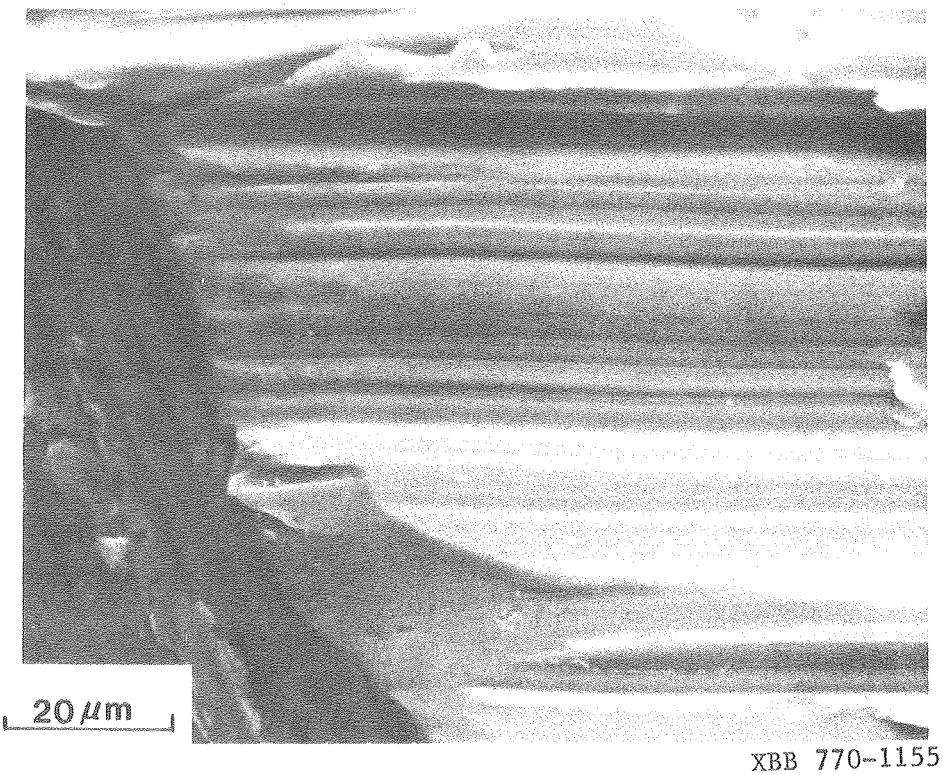

XBB 770-11553

FIGURE 18. 7075-T6 Aluminum Abraded on ~ 115 μm Abrasive

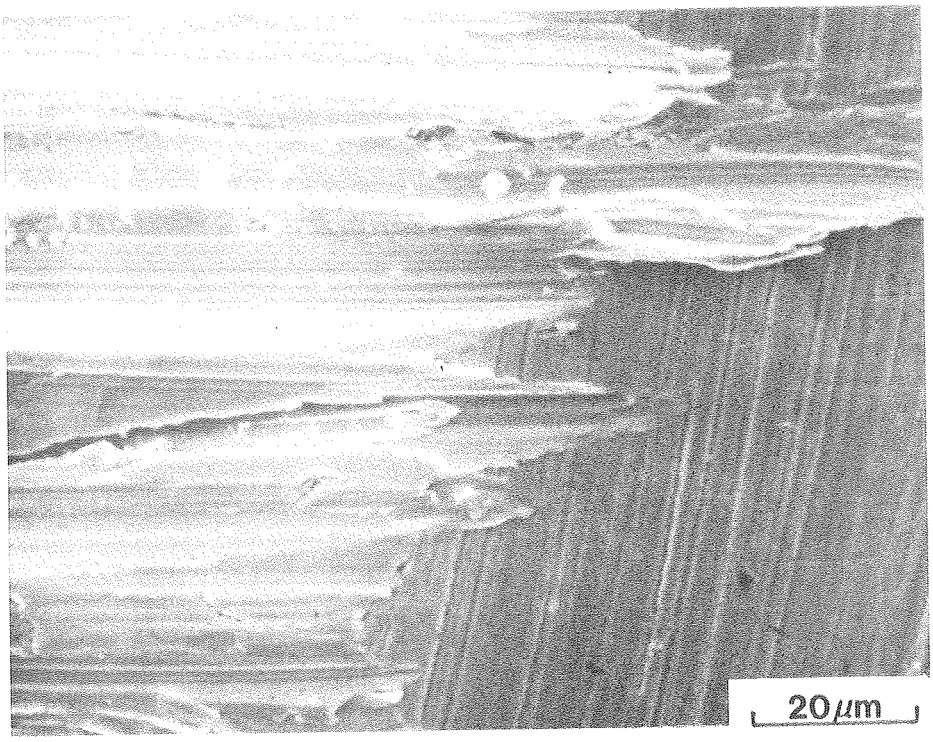

FIGURE 19. 4340 Steel Abraded on ~ 115 μm Abrasive

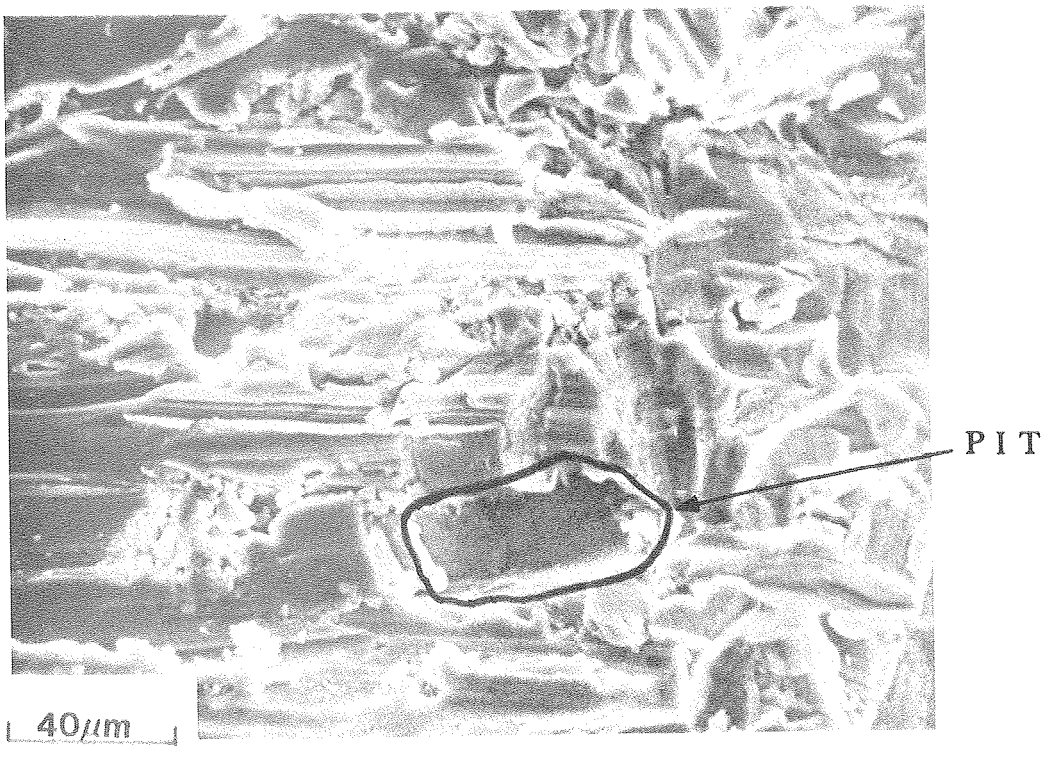

FIGURE 20. Evidence of Cutting, Plastic Flow and Gouging on 7075-T6 Aluminum Specimen Loaded by 500 gm.

XBB 770-11554A

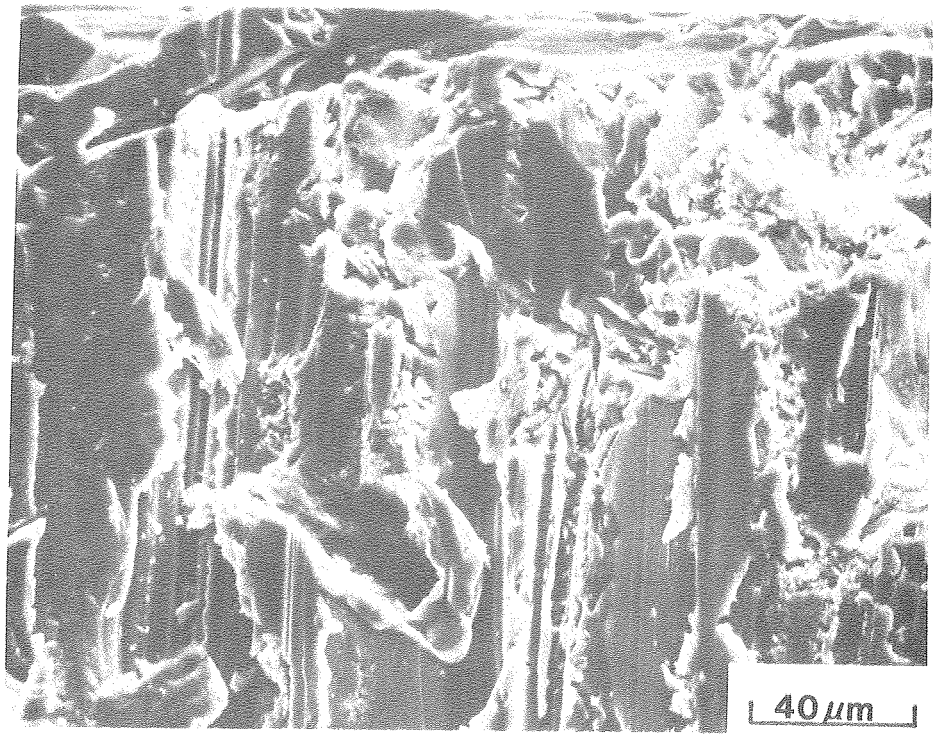

FIGURE 21. 7075-T6 Aluminum (Loaded by 1000 gm) at the Trailing Edge

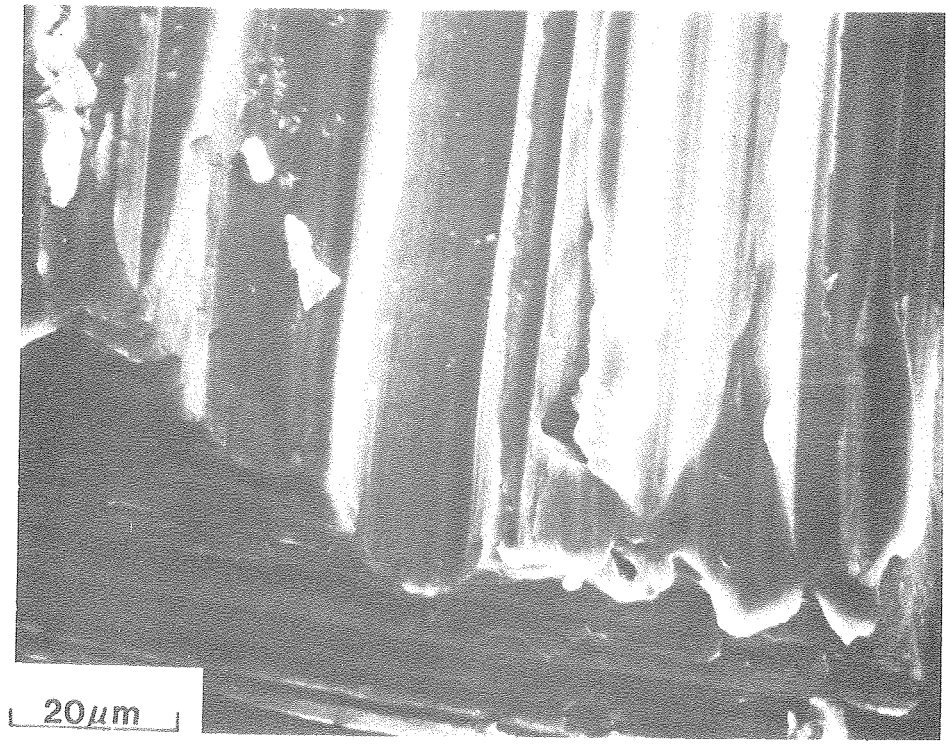

FIGURE 22. 7075-T6 Aluminum (Loaded by 1000 gm) at the Leading Edge.

XBB 770-11555

examines the leading edge of a specimen. Fig. 22 shows the leading edge of the same specimen as shown in Fig. 21. Any cutting chips which may be formed at the leading edge are either removed or continued to the trailing edge.

It is also interesting to compare Fig. 22 and Fig. 18. Both specimens were abraded under the same conditions with the exception that the load of that in Fig. 22 is twice that of Fig. 18. Fig. 22 shows much overlapping of the grooves, possibly due to the increased number of abrasive grains contacting the surface and actually deforming it. Since there are more contacting grains over the same area, the grooves are much closer and overlap to a much greater extent than for lighter loads.

Figs. 23 and 24 are of a 7075 Al specimen which has been cross-sectioned transverse to the abrading direction. The figures show cutting, as seen in the V-shaped grooves, and ploughing where the material from one groove has been extruded over the top of a neighboring groove.

Fig. 25 shows a SiC abrasive particle which is embedded in the specimen. Johnson[15] has studied this and found that some embedded particles may lie beneath the surface. If the embedded particle protrudes above the surface, it will be exposed to other abrasive grains still attached to the paper. As it is pushed along, large pits may form (Fig. 26).

Although this may appear to be strictly a three-body wear phenomena, this type of interaction is bound to occur in two-body abrasion as the abrasive particles are fractured or pulled loose.

Figs. 27 and 28 show another form of degradation caused by loose particles. In this case, what probably occurred is that the loose abrasive particle did not become embedded in the soft material as in the case

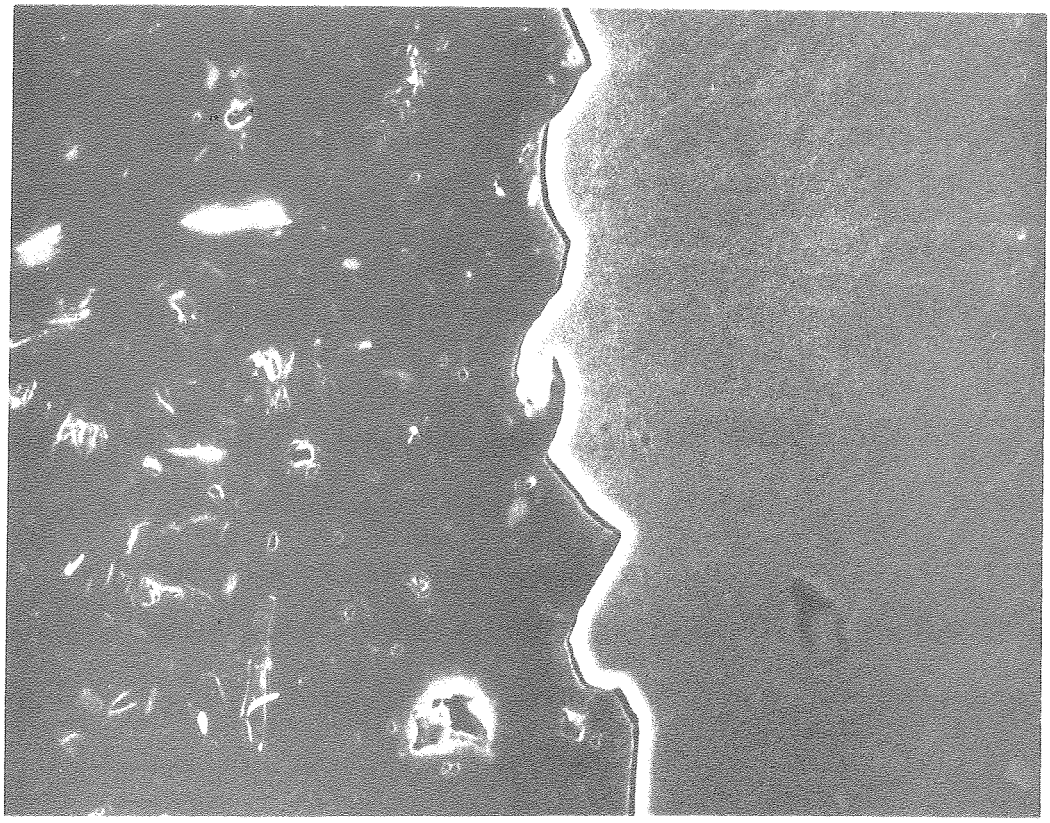

FIGURE 24. 7075-T6 Aluminum Cross-Sectioned Transverse to Abrading Direction.

FIGURE 23. 7075-T6 Aluminum Cross-Sectioned Transverse to Abrading Direction.

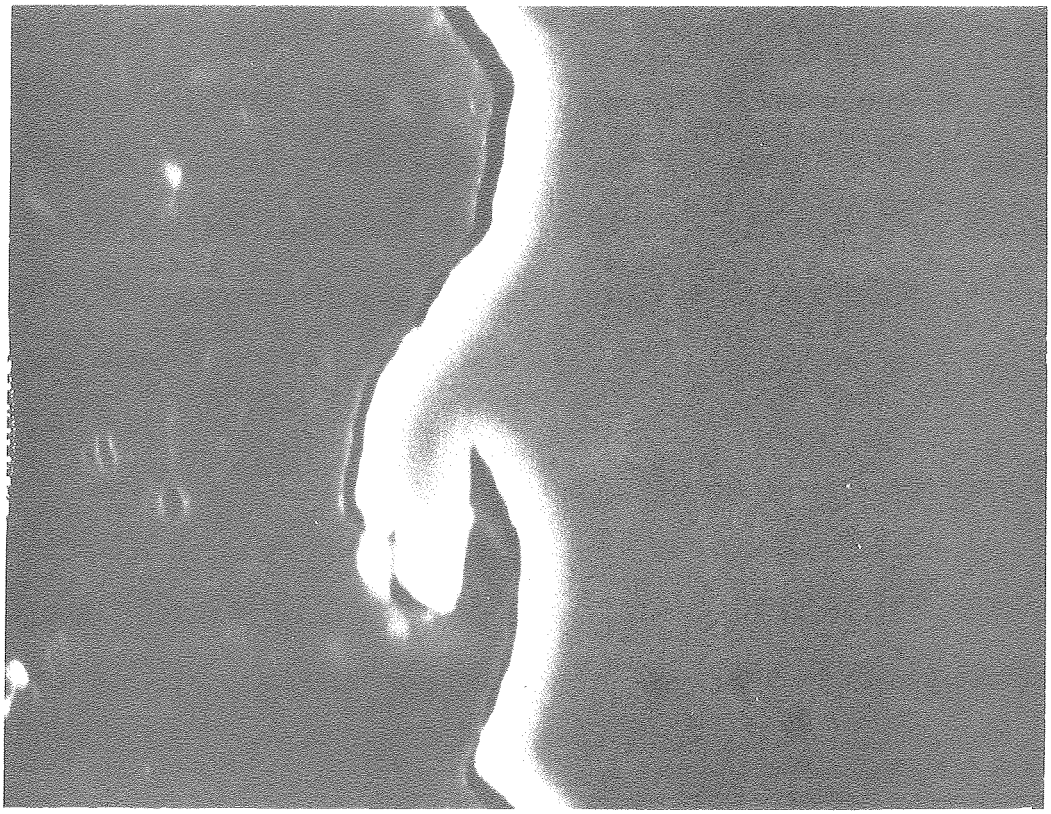

XBB 785-5073

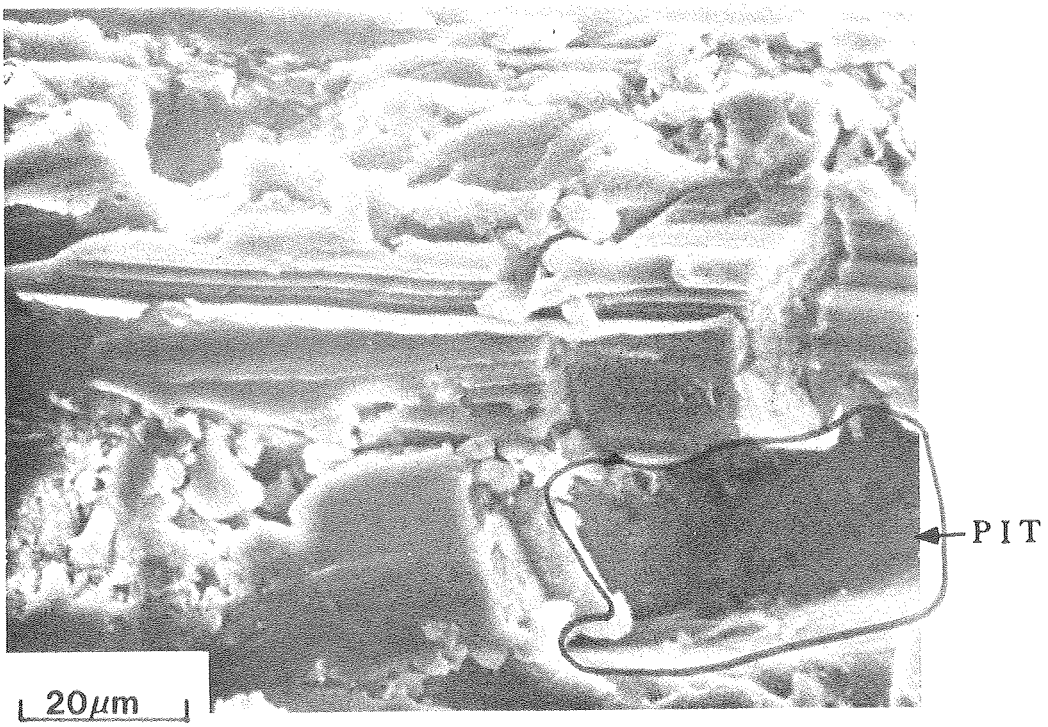

FIGURE 26. Large Pit Formed in 7075-T6 Aluminum

FIGURE 25. Embedded SiC Abrasive Particle

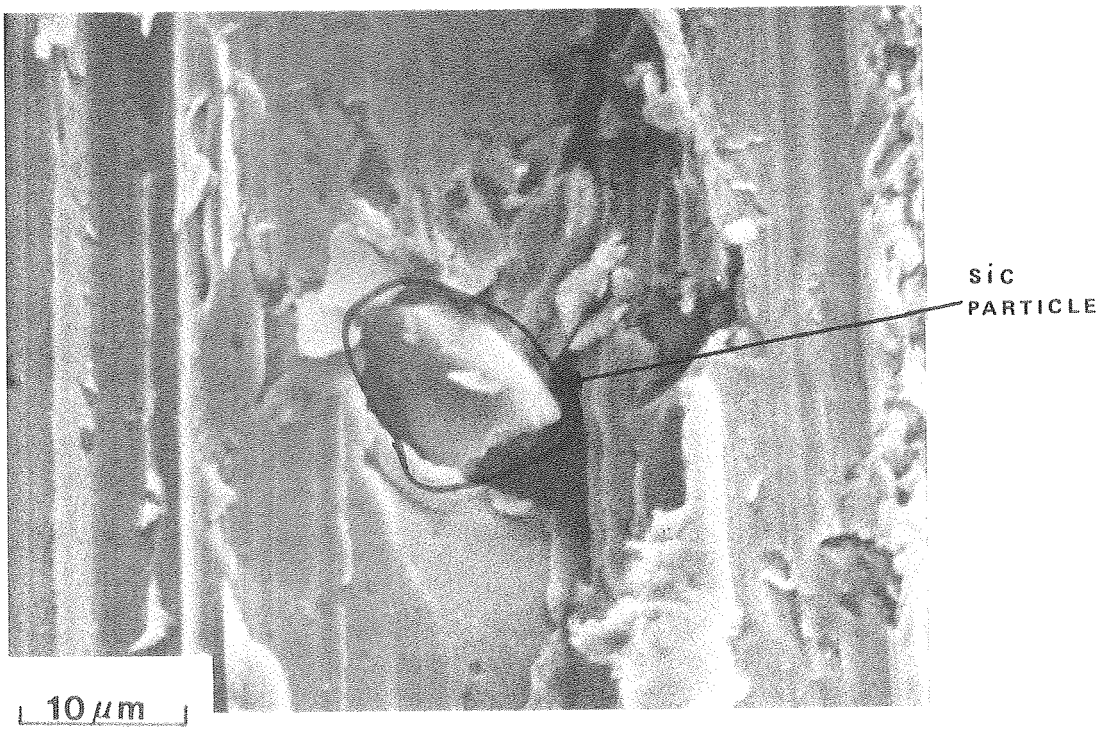

XBB 770-11556A

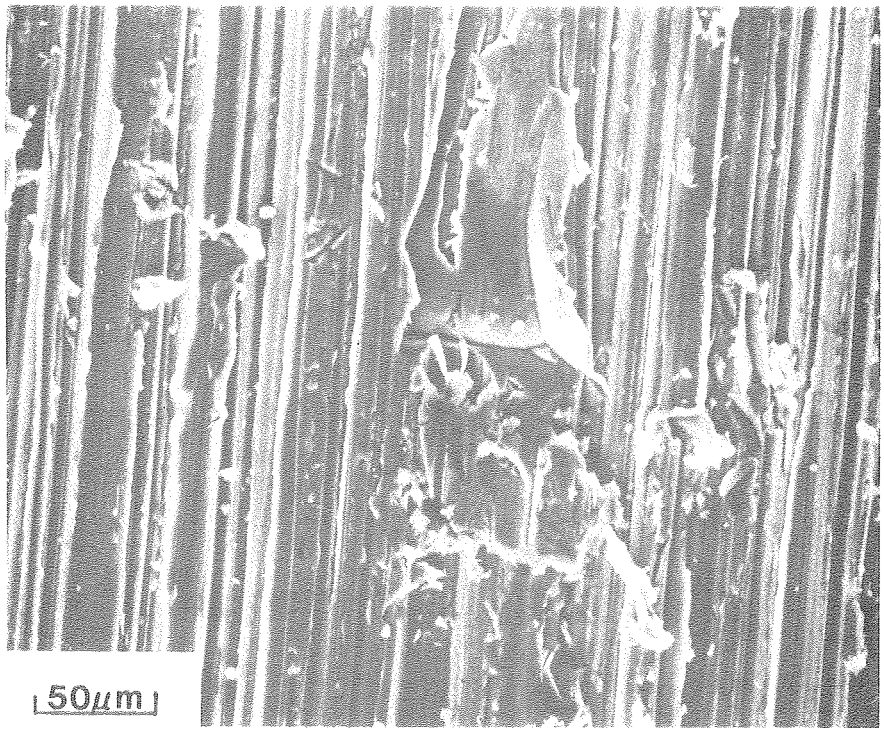

FIGURE 27. Evidence of Plastic Flow in Gouging.

FIGURE 28. Larger Magnification of Figure 27.

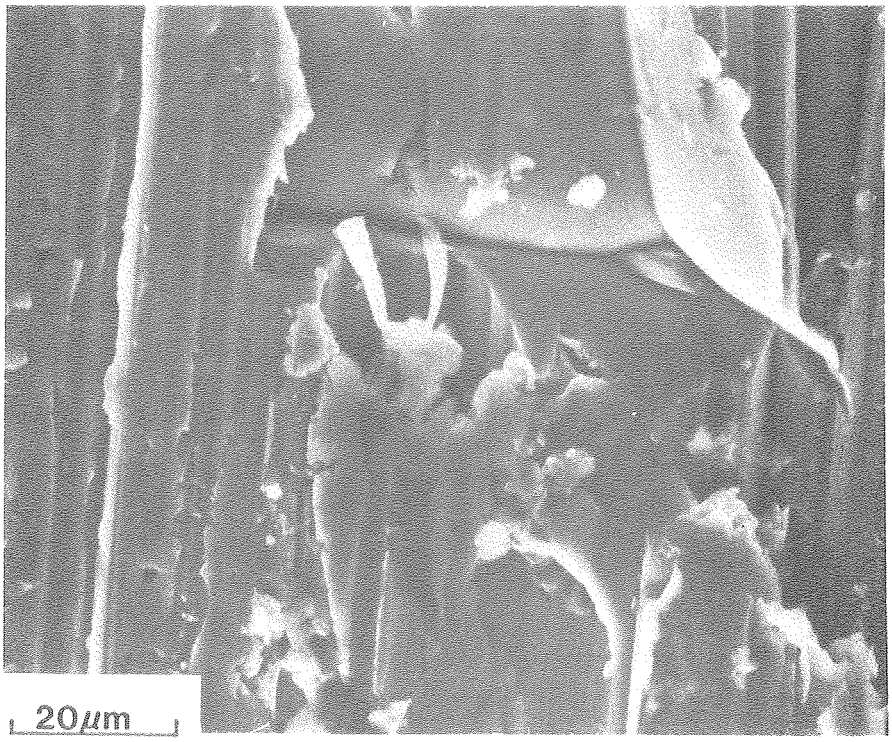

XBB 770-11558

where deep gouges were formed. Rather, the loose abrasive particle rolled along causing a large plastically distorted region. The abrasive grain size for this specimen was ~ 50 μm, which is approximately the width of the pit. By comparing the size of this pit to the surrounding grooves, one can see that only the tip of an abrasive particle contacts the base metal in a two-body situation.

Figs. 29 and 30 are good examples of the chip cutting mechanism which Mulhearn and Samuels concluded was the most effective removal process.

D. Modelling of Two-Body Wear

The development of an analytical model for two-body abrasive wear requires that a mechanism or mechanisms be defined that are conducive to analytical representation such as the concept of micro-cutting developed by Finnie[13] to account for low impingement angle erosion behavior. The mechanisms of material movement that have been observed in two-body wear are:

1. ploughing or extrusion of material ahead of and alongside the track of abrasive particles through the material being abraded (Fig. 22);

2. micro-machining of chips of material from the surface of the abraded material (Fig. 30);

3. embedment of abrasive particles that have separated from the abrasive disc in the surface of the abraded material protecting the material under it (Fig. 25);

4. gouging out of vulnerable partially embedded abrasive particles by collision with subsequent particles still bonded to the abrasive disc, removing abraded material with them to form pits (Figs. 20, 26);

5. abraded material removed upstream adhering to downstream surfaces, adding to its surface and protecting it (Fig. 21);

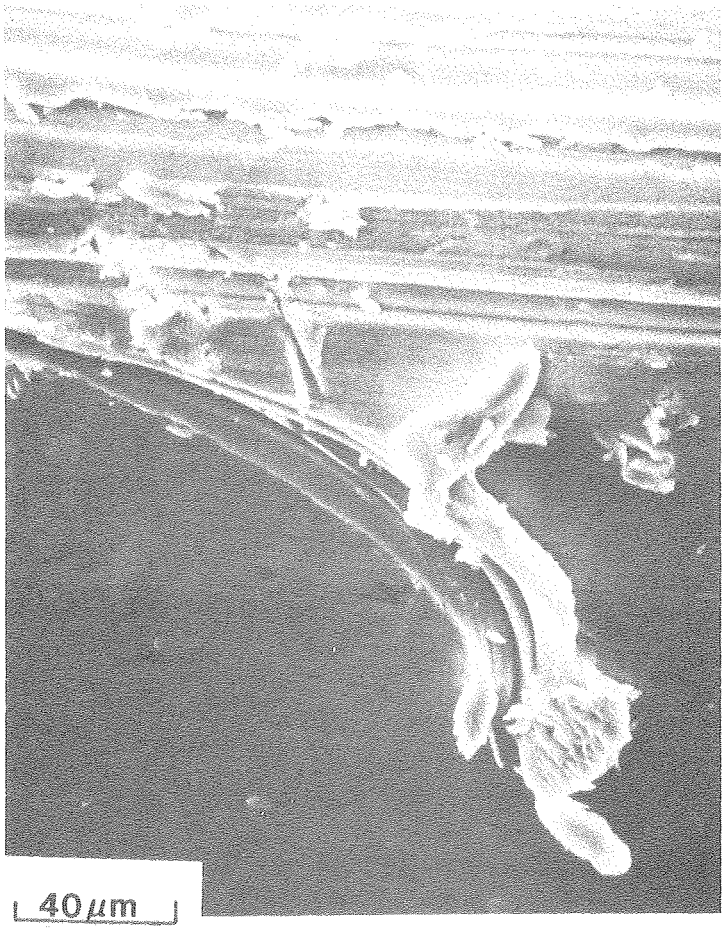

FIGURE 29. Cutting Chip Formation in 7075-T6 Al.

FIGURE 30. Example of Cutting Chip in 7075-T6 Aluminum.

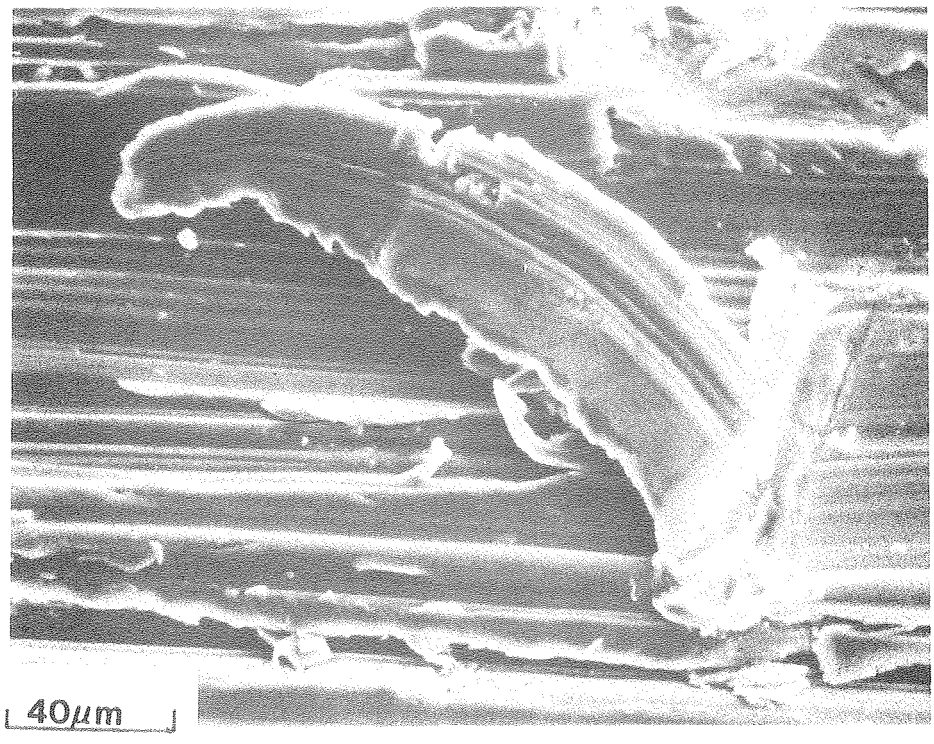

XBB 770-11557

6. adhered upstream material taking welded-on downstream material with it when it is abraded off the surface (Figs. 20, 21).

It is difficult to establish a single mechanism or even a number of mechanisms that can be addressed analytically that would adequately represent all of the above active mechanisms.

As an alternative, one can look for material property variations that directly relate to wear rate as has been done in this investigation, i.e., hardness, yield strength, fracture toughness; and establish a simple dependence ratio embodying the material property that shows a regular relationship to the wear rate. The use of a coefficient of proportionality completes the analytical representation of the relationship. Kruschov did this for hardness and the modulus of elasticity E in reference (1), developing simple and effective equations for each property for relating pure or annealed metal behavior to wear resistance.

$$\varepsilon = bH \qquad \text{and} \qquad \varepsilon = C_1 E^{1.3}$$

where ε = relative wear resistance

b = coefficient of proportionality for H

H = diamond indentation hardness

C_1 = coefficient for proportionality for E

E = modulus of elasticity

Similar expressions can be used with the data obtained in this investigation.

It is our intent to develop a model that represents an integration of several mechanisms and pertinent material properties and not simply a straight line plot correlation of a single property such as hardness with

wear resistance. Fracture toughness was investigated to determine how its integration of plastic behavior of materials might indicate a direction that model development could take. Fig. 12, which shows the relationship of fracture toughness and wear resistance may provide a clue to modelling wear behavior.

It has been observed in solid particle erosion of metals[16] that the wear rate could be related to the relative proportion and distribution of hard second phase material in the softer matrix phase. The greater the concentration of the hard phase, resulting in more continuous ductile matrix phase, the more resistant to metal loss the alloy was. In that investigation Al-4.75%Cu alloy was used; its microstructure is somewhat similar to that of 7075 Al used in this study.

If one looks at the curve of fracture toughness vs. wear resistance of 7075 Al (Fig. 12) it can be seen that there are two distinct behaviors, one for the overaged material where the harder phase precipitate is consolidating with increasing aging temperature, and the other for the underaged material, which is progressing towards maximum distribution of the hard phase with a minimum of soft, matrix phase between hard precipitate material. The overaged material has the largest amount of ductile matrix phase between the hard precipitate. It can be seen in Fig. 12 that differences in the fracture toughness of the overaged material cause significantly greater changes in the wear resistance than do changes in the underaged material. With further work, it is hoped that the distribution of softer, ductile matrix material in a multi-phase alloy can be correlated with wear resistance.

IV. CONCLUSIONS

As a means of estimating the abrasive wear resistance of a material by its mechanical properties, hardness and yield strength seem to offer the best correlations. However, it must be kept in mind that the Vicker's Hardness test is a measure of flow properties of a material at low strains whereas abrasion involves high strains. For annealed, pure, FCC metals the stress-strain curves should be similar; therefore, one would expect a good correlation between wear resistance and the Vicker's Hardness. For cold-worked or heat-treated materials such as 4340 steel, the stress-strain curves are much flatter than for annealed metals. This implies that the flow pressure at high strains would be overestimated by the Vicker's Hardness. Thus, the increase in wear resistance for a given increase in the Vicker's Hardness is less for cold-worked or heat-treated materials than for pure annealed metals. This is seen as the flatter slope in Fig. 16.

The 4340 steel demonstrates a level of correlation of the wear resistance to the fracture toughness. The 7075 Al has two distinct relationships between wear resistance and fracture toughness, each related to a type of microstructure.

The observed mechanisms of abrasive wear are plastic flow, cutting and gouging. All three mechanisms are likely to exist during two-body abrasion; however, one may dominate. The extent of gouging depends on the fracture properties of the abrasive and the manner in which it is fixed to the abrasive surface in the two-body condition. Whether cutting or plastic flow occurs depends largely on the angle of attack of the abrasive particles. Therefore, for situations where the abrasive is

very much harder than the material being tested, the dominant wear mechanism probably depends primarily on the characteristics of the abrasive (i.e. angle of attack, fracture behavior, bonding technique).

The development of an analytical model for two-body abrasive wear will require the integration of several mechanisms of material movement-removal with pertinent material properties and morphologies.

REFERENCES

1. Kruschov, M.M., "Principles of Abrasive Wear," Wear, (1974) 69-88.

2. Rabinowicz, E., Friction and Wear of Materials, John Wiley and Sons, New York, 1965.

3. Mulhearn, T.O. and Samuels, L.E., "The Abrasion of Metals: A Model of the Process," Wear, 5 (1962) 478-498.

4. Bowden, F.P. and Tabor, D., The Friction and Lubrication of Solids, Oxford University Press, London, 1964.

5. Larsen-Badse, J., "Some Effects of Specimen Size on Abrasive Wear," Wear, 19 (1972) 27-35.

6. Larsen-Badse, J., "Influence of Grit Size on the Groove Formation During Sliding Abrasion," Wear, 11 (1968) 213-222.

7. Date, S.W. and Malkin, S., "Effects of Grit Size on Abrasion with Coated Abrasives," Wear, 40 (1976) 223-235.

8. Goddard, J. and Wilman, H., "A Theory of Friction and Wear During the Abrasion of Metals." Wear, 5 (1962) 114-135.

9. Pujari, V.K., "An Improved Method for Fracture Toughness Evaluation in the Linear Elastic Range and a Comparison with Elastic-Plastic Data Obtained with Smaller Specimens," PhD Dissertation, University of California, Berkeley.

10. Shenai, K.P., "A Study of the Influence of Underaging on Mechanical Properties of 7075 Aluminum Alloy," M.S. Report, University of California, Berkeley.

11. Horn, R.M. and Ritchie, R.O., paper submitted to Met. Trans.

12. Throop, J.F. and Miller, G.A., "Optimum Fatigue Crack Resistance," Achievement of High Fatigue Resistance in Metals and Alloys, ASTM STP 467, American Socity for Testing and Materials (1970) 157.

13. Finnie, I., "Some Observations on the Erosion of Ductile Metals," Wear, 19 (1972) 81-90.

14. Aghan, R.L. and Samuels, L.E., "Mechanisms of Abrasive Polishing," Wear, 16 (1970) 293-301.

15. Johnson, R.W., "A Study of the Pickup of Abrasive Particles During Abrasion of Annealed Aluminum on Silicon Carbide Abrasive Papers," Wear, 16 (1970) 351-358.

16. Brass, L.M., "The Effects of Microstructure of Ductile Alloys on Solid Particle Erosions, M.S. Thesis, University of California, Berkeley.

TABLE I: Mechanical properties of 7075 Aluminum Wear Specimens

	Aging Temperature (°F)	Vicker's Hardness (Kg/mm^2)	Yield Strength (Ksi)	Fracture Toughness K_c ($Ksi-in^{1/2}$)
Underaged:	202	158.0	66.8	61
	209	163.0	68.6	58
	223	167.0	69.1	51
Overaged:	250	180.5	78.5	23.0
	254	181.0	77.1	23.0
	264	179.5	76.8	23.5
	305	167.0	73.5	25.0
	318	134.0	70.4	25.0
	332	122.5	67.5	26.0
	359	106.0	50.2	29.0
	371	102.0	46.2	31

Yield strength and fracture toughness data for overaged material obtained from Reference 9.

Fracture toughness data for underaged material from Reference 10.

TABLE II: Mechanical Properties of 4340 Steel Wear Specimens

Tempering Temperature (°C)	Vicker's Hardness (Kg/mm^2)	Yield Strength (Ksi)	Fracture Toughness K_{Ic} ($Ksi\text{-}in^{1/2}$)
200	602	233	39
350	498	208	40
500	407	164	89
650	318	111	160

Yield strength data from Reference 11.

Fracture toughness data from Reference 12.

TABLE III: Abrasive Wear Constants reported by Rabinowicz[2]

Investigator/Material Studied	Abrasive Size (μm)	$k(x10^{-3})$
Kruschov/Several	80	24
Avient, et al/Several	40-150	120
Spurr, et al/Several	110	150

FIGURE CAPTIONS:

1. Two-Body and Three-Body Abrasion
2. Summary of Data by Kruschov
3. Simple Model of Abrasion by Rabinowicz
4. Pin-on-Disc Abrasion Tester
5. Overall View of Dry Abrasive Wear Tester
6. View of Test Area of Dry, Abrasive Wear Tester
7. Closeup of Pin and Abrasive Disc
8. Effect of Load on Wear Rate of 7075-T6 Aluminum
9. Effect of Abrasive Particle Size on Wear Rate of 7075-T6 Al.
10. Wear Resistance of 7075 Al vs. Hardness
11. Wear Resistance of 7075 Al vs. Yield Strength
12. Wear Resistance of 7075 Al vs. Fracture Toughness
13. Wear Resistance of 4340 Steel vs. Hardness
14. Wear Resistance of 4340 Steel vs. Yield Strength
15. Wear Resistance of 4340 Steel vs. Fracture Toughness
16. Comparison of Wear Resistance of 7075 Al and 4340 Steel
17. 7075-T6 Al Abraded on ~ 14 μm Abrasive
18. 7075-T6 Al Abraded on ~ 115 μm Abrasive
19. 4340 Steel Abraded on ~ 115 μm Abrasive
20. Evidence of Cutting, Plastic Flow and Gouging on 7075-T6 Al Specimen loaded by 500 gm.
21. 7075-T6 Al (loaded by 1000 gm) at the Trailing Edge
22. 7075-T6 Al (loaded by 1000 gm) at the Leading Edge
23. 7075-T6 Al Cross-Sectioned Transverse to Abrading Direction
24. 7075-T6 Al Cross-Sectioned Transverse to Abrading Direction
25. Embedded SiC Abrasive Particle
26. Large Pit Formed in 7075-T6 Al
27. Evidence of Plastic Flow in Gouging
28. Larger Magnification of Figure 27
29. Cutting Chip Formation on 7075-T6 Al
30. Example of Cutting Chip in 7075-T6 Aluminum

This report was done with support from the United States Energy Research and Development Administration. Any conclusions or opinions expressed in this report represent solely those of the author(s) and not necessarily those of The Regents of the University of California, the Lawrence Berkeley Laboratory or the United States Energy Research and Development Administration.